Published by
NIGERIAN SOCIETY OF PHYSICAL SCIENCES
Available online @ https://journal.nsps.org.ng/index.php/jnsps

J. Nig. Soc. Phys. Sci. 8 (2026) 3502

Journal of the Nigerian Society of Physical Sciences

Modeling and stability analysis of a fractional-order tuberculosis model with different exposed populations progressing to infection

Muhammad Farman[a,b,c], Kottakkaran Sooppy Nisar[d,*]

[a]Faculty of Arts and Sciences, Department of Mathematics, Near East University, Mersin 10, Nicosia 99138, Turkey
[b]Faculty of Medicine, Department of Biostatistics and Medical Informatics, Karadeniz Technical University, Trabzon, Turkey
[c]International Center for Interdisciplinary Research in Sciences, The University of Lahore, Lahore, Pakistan
[d]Department of Mathematics, College of Science and Humanities in Al-Kharj, Prince Sattam Bin Abdulaziz University, Al-Kharj 11942, Saudi Arabia

Abstract

This study develops a fractional-order mathematical model based on the Atangana–Baleanu–Caputo (ABC) operator to investigate the transmission dynamics of tuberculosis (TB). The framework incorporates memory and nonlocal effects to represent the spread and progression of TB within a population. The first derivative of a Lyapunov function is used to evaluate the infection locally and globally within the fractional-order model. The model satisfies the essential mathematical properties of positivity, boundedness, existence, and uniqueness of solutions, thereby establishing its biological and mathematical well-posedness. Fixed-point theory is used to analyze the model and bound its solution. The analysis establishes local and global stability conditions and identifies the parameters that most strongly affect disease transmission. An advanced numerical method is used to obtain approximate solutions of the fractional-order system and evaluate the effect of the fractional-order parameter. Numerical simulations show that decreasing the fractional-order parameter enhances memory effects and produces smoother convergence toward equilibrium states than the classical integer-order model. The results indicate that the fractional-order framework provides a useful representation of TB dynamics and may support the understanding and control of TB transmission.

DOI: 10.46481/jnsps.2026.3502

Keywords: Tuberculosis model, Well-posedness, Basic reproduction number, Lyapunov stability, Simulation

Article History:
Received: 08 May 2026
Received in revised form: 13 July 2026
Accepted for publication: 18 July 2026
Available online: 10 August 2026

Communicated by: B. J. Falaye

1. Introduction

Tuberculosis (TB) is an infectious disease frequently caused by *Mycobacterium tuberculosis*. Despite frequently affecting the lungs, TB may impair other organs as well. Latent TB is the term used to describe an infection that is undetected. Nearly 50% of patients with active illness, which results from around 10% of latent infections, die if untreated. A chronic cough that generates blood-tinged mucus, fever, weight loss, and night sweats are classic indicators of active tuberculosis. Previously, the disease was called consumption because of its association with weight loss. Infections in different organs can cause a wide range of symptoms. Pulmonary tuberculosis most commonly affects the lungs, but it can affect any part of the body. Extra-pulmonary tuberculosis is the term for TB that develops outside of the lungs, although it can coexist with pulmonary tuberculosis. The paper also examines the potential root causes of these

*Corresponding author Tel. No.: +966-563456976.
Email address: n.sooppy@psau.edu.sa (Kottakkaran Sooppy Nisar)

issues, including socioeconomic barriers to care, ineffective tuberculosis services, particularly in underserved areas, a lack of collaboration between healthcare facilities, and a lack of political will and financial support for TB control on the part of local governments. The study concludes with a review of the potential and difficulties that TB control faces and offers suggestions for further initiatives and research [1]. The recent assessment found that one-third of those with TB illness may not have received treatment or disease notification. Not all TB patients are being recorded by the ETR. Additionally, the TB Surveillance System's data sources differ in their completeness and trustworthiness of information for patients with a TB record. Urgent action is required to enhance the integrity of surveillance data and guarantee that all diagnosed individuals are handled and treated [2]. The HIV pandemic, immigration, and treatment resistance have all been linked to the comeback of tuberculosis (TB) in Western nations. Multidrug-resistant tuberculosis is caused by two main factors: either drug-resistant bacteria from previous therapy were chosen, or multidrug-resistant Mycobacterium tuberculosis (MT) strains were introduced in new patients. In Europe, the biggest predictor of MDR-TB was prior therapy. A thorough investigation of the causes of insufficient therapy might enhance control measures. It is necessary to reevaluate the risk of MDR-TB in individuals who were born abroad while accounting for any prior therapy [3]. In addition to regular health information systems, designated hospitals, health insurance firms, key informant interviews, and focus groups with pertinent key stakeholders, data was gathered through TB and MDR-TB patient questionnaires. The use of TB services and anti-TB medications and the factors that influence them as socioeconomic and health systems develop are among the main topics covered in this collection of papers. The expenses of TB treatment and the financial strain on TB patients are other significant subjects, as is the impact of China's health insurance policies on financial stability [4]. Research should be specific about the study's context, the number of cases included, the recruiting time, and the clustering criteria that were employed. The clustering data ought to be broken down at least by age, sex, and immigrant status. Studies should include a significant portion of all cases in the population, be conducted in conjunction with traditional epidemiological investigations of contacts (if possible), and provide data on the incidence of tuberculosis in the population as well as patient characteristics such as age, sex, HIV status, drug sensitivity, and social and ethnic group [5]. Tsai *et al.* [6] used gold nanoparticles and an analytical platform based on paper to develop a colorimetric sensing method for diagnosing tuberculosis. Using the surface plasmon resonance approach, the authors were able to monitor color changes in a gold nanoparticle colloid based on the outcomes of single-stranded DNA probe molecules hybridizing with certain double-stranded TB sequences. Simply detecting how the hybridization process alters the nanoparticles' surface charge density, which leads to varying degrees of aggregation, yields the necessary DNA analysis. James *et al.* discovered that the chance of contracting an active illness following exposure to the TB bacilli is a two-stage process that is influenced by both endogenous and extrinsic risk factors. A person's proximity to an infectious TB case and the bacillary load in their sputum are two critical external factors that can exacerbate the shift from exposure to infection. The development of infection into active tuberculosis is driven by similar internal mechanisms. Emerging risk factors, like cigarette smoking, alcohol use, diabetes, indoor air pollution, and immunosuppressive drug usage, have a big influence on people and communities in addition to known risk factors [7].

It has been demonstrated that these mathematical models are helpful in solving scientific and technological issues [8–11]. The primary goal of the aforementioned studies is to investigate tuberculosis infections from multiple perspectives by using fractional operators. Researchers from around the world are also considered for solving scientific and technical difficulties utilizing mathematical models of fractional operators. A few months after the pandemic began, a number of models for analyzing the dynamics of this disease in different parts of the world were available in the literature [12–16]. Using a smooth kernel that may represent the temporal and spatial variables in two different ways, Caputo and Fabrizio created a novel definition of the fractional derivative. The Laplace transform is appropriate for the first since it operates on time variables. The non-local fractional derivative that connects the second definition to the spatial variables makes working with the Fourier transform more practical [17, 18]. A Caputo fractional-order tuberculosis model [19] was developed and validated against real epidemiological data, demonstrating the improved capability of fractional calculus to capture disease transmission dynamics and predict outbreak trends. A comprehensive fractional-order tuberculosis model incorporating treatment intervention was analyzed to investigate disease dynamics [20], stability behavior, and the effectiveness of control strategies in reducing TB transmission. The dynamics of tuberculosis within a population [21] cannot be adequately represented by a single infectious class. Therefore, this study develops a compartmental model encompassing latent, active, and drug-resistant populations to better capture tuberculosis dynamics in a community. The study [22] proposed an age-structured deterministic model governing the transmission dynamics and control of TB in the presence of vaccination integrated into the eligible population. A fractional-order bilingualism model [23] employs the Mittag–Leffler kernel, demonstrating the effectiveness of non-singular fractional operators in capturing memory effects and complex language interaction dynamics. A fractional-order modeling framework was utilized to investigate the dynamics of insect pests and nematodes in pine forests [24], providing insights into effective forest management and ecological control strategies. Higher-order interactions were incorporated into a spatio-temporal Leslie-Gower predator–prey model to better understand complex ecological dynamics [25], pattern formation, and species coexistence mechanisms.

This study includes the formulation of a tuberculosis transmission model with two exposed populations under the Atangana–Baleanu-Caputo fractional operator. The model's positivity, boundedness, existence, and uniqueness properties are established, while the basic reproduction number and equilibrium stability conditions are rigorously analyzed. In addi-

tion, sensitivity analysis is employed to identify the key epidemiological parameters influencing disease spread. Numerical experiments are performed for different fractional orders to investigate the impact of memory effects on the transmission dynamics and to assess the advantages of the proposed fractional framework over its classical counterpart. Recent studies have demonstrated the usefulness of fractional-order approaches in describing tuberculosis dynamics by incorporating memory effects and hereditary characteristics. Nevertheless, most available models rely on traditional fractional operators and simplified compartmental structures, which may not adequately capture the complexity of disease progression. Moreover, the role of multiple exposed populations in tuberculosis transmission under a fractional framework with a non-singular kernel has received limited attention. Existing investigations are also often restricted to specific mathematical properties, leaving a need for a unified framework that integrates epidemiological analysis with computational assessment. These limitations motivate the development of the present model, which aims to provide a more comprehensive understanding of tuberculosis dynamics through an Atangana–Baleanu-Caputo fractional formulation.

The following are the remaining sections of this research article: A detailed overview of the proposed model is provided in section 3. Section 2 has some basic fractional order derivatives that can be used to solve the epidemiological model. Section 3 provides a generalized version of the model and an analysis of its suggested description, including studies on well-posedness, positivity, and boundedness. Section 4 analyzes the qualitative properties of the model, including the disease-free equilibrium, reproduction number, sensitivity analysis, existence, uniqueness, and stability. Section 5 presents the Adams-Bashforth numerical scheme, while Sections 6 and 7 present the numerical simulations and conclusion, respectively.

2. Basic concepts

We found some important and practical discoveries concerning modern calculus and nonlinear dynamics in [26, 27].

Definition 2.1. The Atangana–Baleanu–Caputo (ABC) fractional derivative, with $\tau \in (0, 1]$ and for function $\omega(t) \in L^1[0, T]$ is given by

$$ {}^{ABC}D_t^{\tau}\omega(t) = \frac{Z(\tau)}{1-\tau}\int_0^t E_{\tau}\left[\frac{-\tau}{1-\tau}(t-\vartheta)\right] \frac{d}{d\vartheta} \times \omega(\vartheta)d\vartheta. \tag{1}$$

The normalization function is $Z(\tau)$, where $Z(0) = Z(1) = 1$. The Mittag–Leffler's function E_τ is clearly defined as

$$E_\tau(y) = \Sigma_{k=0}^{\infty}\frac{y^k}{\Gamma(\tau k+1)}. \tag{2}$$

Definition 2.2. When using the ABC technique, the left-hand side (LHS) of an integral of order $\tau \in (0, T]$ is represented as if $\omega(t) \in L^1(0, T)$ is a function.

$$ {}^{ABC}I_t^{\tau}\omega(t) = \frac{1-\tau}{Z(\tau)}\chi(t) + \frac{\tau}{\Gamma(\tau)Z(\tau)}\int_0^t (t-\vartheta)^{\tau-1}\omega(\vartheta)d\vartheta. \tag{3}$$

Theorem 2.1. Now suppose that U is a closed norm space and $\psi \subset U$ is a convex, closed, and bounded set. Then a continuous function $\Omega : \psi \to \psi$ has at least one stationary point in ψ and $\Omega\psi \subset U$ and $\Omega\psi$ is substantially compact.

3. Tuberculosis fractional-order mathematical model with treatment

Our model of the dynamics of tuberculosis infection is compartmental and deterministic. Scientists are investigating the origins and recurrence of disease outbreaks. We analyze several important features of the compartmental mathematical epidemic model for the spread of viruses proposed by Zhang *et al.* [28]. The set of nonlinear equations that follows represents a plan to treat and eradicate tuberculosis. The proposed framework may be expressed as

$$\begin{cases} {}^{ABC}\mathbb{D}_t^{\tau}S(t) = \Delta - \frac{\beta SI}{N} - \nu S, \\ {}^{ABC}\mathbb{D}_t^{\tau}E_1(t) = \omega\frac{\beta SI}{N} - \chi_1 E_1 + (1-\rho)\delta T, \\ {}^{ABC}\mathbb{D}_t^{\tau}E_2(t) = (1-\omega)\frac{\beta SI}{N} + \varsigma_1 E_1 - \chi_2 E_2, \\ {}^{ABC}\mathbb{D}_t^{\tau}I(t) = \varsigma_2 E_2 + \rho\delta T - \chi_3 I, \\ {}^{ABC}\mathbb{D}_t^{\tau}T(t) = \gamma I - \chi_4 T, \\ {}^{ABC}\mathbb{D}_t^{\tau}R(t) = \phi T - \nu R, \end{cases} \tag{4}$$

let

$$\begin{aligned} \chi_1 &= \nu + \varsigma_1, \\ \chi_2 &= \nu + \varsigma_2, \\ \chi_3 &= \nu + \gamma + \sigma_1, \\ \chi_4 &= \nu + \delta + \sigma_2 + \phi, \end{aligned} \tag{5}$$

where the starting circumstances are

$$S(0) = S^0 \geq 0, E_1(0) = E_1^0 \geq 0, E_2(0) = E_2^0 \geq 0, I(0) = I^0 \geq 0, \tag{6}$$

$$T(0) = T^0 \geq 0, R(0) = R^0 \geq 0. \tag{7}$$

3.1. Model description

The proposed model splits the whole population N into six compartments at a given time t. In order to analyze the dynamics of tuberculosis, we developed a fractional-order mathematical model that takes into account six compartment populations and employs efficient personnel. $S(t)$ denotes the susceptible segment of the population at time t; the slow-exposed group is denoted by $E_1(t)$, the fast-exposed group by $E_2(t)$, the infected group by $I(t)$, the treatment group by $T(t)$, and the recovered group by $R(t)$. In model (4), after interaction between susceptible and infected persons, a ratio $\omega(0 < \omega < 1)$ of susceptible individuals $S(t)$ joins $E_1(t)$ and a fraction $(1-\omega)$ enters the fast exposed class E_2 directly. Δ and ν denote the birth and death rates, respectively, while β represents the successful transmission coefficient. The disease-induced rates due to disease in

Table 1: Description of the model parameters.

Parameter	Description
Δ	Birth rate
ν	Natural death rate
β	Contact rate
γ	Treatment rate of infectious individuals
ρ	Unsuccessful treatment rate
σ_1	Disease-induced death rate in the infectious class (I)
σ_2	Disease-induced death rate during treatment (T)
ς_1	Transition rate from exposed class E_1 to E_2
ς_2	Progression rate from exposed class E_2 to infectious class I
δ	Re-entry rate of treated individuals into I or exposed classes after treatment failure
ω	Fraction of susceptible individuals entering the slow exposed class E_1 after contact with infectious individuals
ϕ	Recovery (restoration) rate

compartments I and T are given by σ_1 and σ_2, respectively. The rate of progression from E_1 to E_2 is ς_1 and from E_2 to I is ς_2. For the infected individuals, the per capita treatment rate is represented by γ, and δ is the rate at which individuals quit the $T(t)$ compartment due to incomplete treatment. The fraction of individuals leaving the treatment class T that reenters the infected class I is denoted by $\rho\delta T$, and the remaining $\delta T(1-\rho)$ rejoins the slow exposed class depending on the treatment state of the individuals. The evolution rate is ϕ, at which treated T becomes recovered R. The parameter $\rho(0 < \rho < 1)$ in $(1-\rho)\delta$ represents the ratio of drug-defiant people in compartment T. Table 1 provides information on the parameters of the suggested model.

Consequently, the overall population is determined by

$$\mathbb{N}(t) = S(t) + E_1(t) + I(t) + E_2(t) + T(t) + R(t). \tag{8}$$

3.2. Well-posedness

In this section, we analyze the temporal context and spatial domain in which the responses of the proposed model hold historical significance. All solutions and recommended parameters are advantageous for each t, as demonstrated in our earlier findings. We know that, for $t > 0$:

$${}^{ABC}\mathbb{D}_t^{\tau}\mathbb{N}(t) = \Delta - \nu\mathbb{N}(t) - \sigma_1 I(t) - \sigma_2 T(t), \tag{9}$$

we want $\mathbb{N}(t)$ to be an increasing function, such that ${}^{ABC}\mathbb{D}_t^{\tau}\mathbb{N}(t) > 0$.

$${}^{ABC}\mathbb{D}_t^{\tau}\mathbb{N}(t) \leq \Delta - \nu\mathbb{N}(t), \qquad \mathbb{N}(t) \leq \frac{\Delta}{\nu}. \tag{10}$$

The aforementioned disparity is referred to as the necessary population level in the literature. Consequently, we derive that the acknowledged set of solutions for the proposed model should be limited to

$$\Omega = \left\{ \begin{array}{l} (S, E_1, I, E_2, T, R) \in R_+^6 : \\ S + E_1 + I + E_2 + T + R = \mathbb{N} < \frac{\Delta}{\nu} \end{array} \right\}. \tag{11}$$

In this case, the faces of the positive cone of R_+^6 are likewise found in the lower dimensions. Realistically speaking, we rule out the circumstance where ${}^{ABC}\mathbb{D}_t^{\tau}\mathbb{N}(t) \geq 0$. The host population may eventually drop to its carrying capacity as a result of this.

3.3. Positivity and boundedness of the proposed model solutions

To demonstrate the transparency of all results and their ability to address global concerns, we provide a detailed description of the fundamental components below. This section examines the various ways in which we can obtain the desired value of the structure.

Let's start with class $E_1(t)$:

$$E_1(t) \geq E_1^o e^{-(\nu+\varsigma_1)t}, \quad \forall t \geq 0, \tag{12}$$

The function $E_2(t)$ has the following inequality.

$$E_2(t) \geq E_2^o e^{-(\nu+\varsigma_2)t}, \quad \forall t \geq 0, \tag{13}$$

$$I(t) \geq I^o e^{-(\nu+\gamma+\sigma_1)t}, \quad \forall t \geq 0, \tag{14}$$

$$T(t) \geq T^o e^{-(\nu+\delta+\sigma_2+\phi)t}, \quad \forall t \geq 0, \tag{15}$$

and

$$R(t) \geq R^o e^{-(\nu)t}, \quad \forall t \geq 0. \tag{16}$$

We will establish the norm:

$$\|\lambda\|_\infty = sup_{t\in D_\lambda}|\lambda(t)|, \tag{17}$$

where D_λ denotes $\lambda' s$ domain. Eq. (17) is used to determine the following discrepancy for the category $S(t)$.

$$\begin{aligned} S(t) &= \Delta - \frac{\beta S I}{N} - S\nu, \ \forall t \geq 0 \\ &\geq -(\nu + \frac{\beta|I|}{|N|})S, \ \forall t \geq 0 \\ &\geq -(\nu + \frac{\beta \sup_{t\in D_I}|I|}{\sup_{t\in D_N}|N|})S, \ \forall t \geq 0 \\ &\geq -(\nu + \frac{\beta\|I\|_\infty}{\|N\|_\infty})S, \ \forall t \geq 0. \end{aligned} \tag{18}$$

Using the positivity of the state variables and the fact that

$$\frac{I(t)}{N(t)} \leq \frac{\|I\|_\infty}{\|N\|_\infty}, \tag{19}$$

we obtain

$${}^{ABC}D_t^{\tau}S(t) = \Delta - \frac{\beta S I}{N} - \nu S \geq -\left(\nu + \frac{\beta\|I\|_\infty}{\|N\|_\infty}\right)S(t). \tag{20}$$

By the comparison principle for fractional differential equations, it follows that

$$S(t) \geq S(0)\, E_\tau\left(-\left(\nu + \frac{\beta\|I\|_\infty}{\|N\|_\infty}\right)t^\tau\right) \geq 0, \qquad t \geq 0, \tag{21}$$

where $E_\tau(\cdot)$ denotes the Mittag–Leffler function. Therefore, $S(t)$ remains nonnegative for all $t \geq 0$ whenever $S(0) > 0$. By applying the same argument to the remaining compartments, we conclude that all state variables remain nonnegative in the feasible region.

4. Qualitative analysis of the proposed model

To gain a deeper comprehension of its characteristics and the processes influencing the dynamics of the spread of TB. The proposed scheme of TB with therapy, which is symbolized by (4), is currently undergoing a qualitative examination.

Setting ${}^{ABC}\mathbb{D}_t^\tau S(t) = {}^{ABC}\mathbb{D}_t^\tau E_1(t) = {}^{ABC}\mathbb{D}_t^\tau E_2(t) = {}^{ABC}\mathbb{D}_t^\tau I(t) = {}^{ABC}\mathbb{D}_t^\tau T(t) = {}^{ABC}\mathbb{D}_t^\tau R(t) = 0$ results in the system's equilibrium points. We have two equilibrium points:

- Disease-free equilibrium:

$$\mathcal{E}^0 = \left\{\frac{\Delta}{\nu}, 0, 0, 0, 0, 0\right\} \tag{22}$$

- Endemic equilibrium:

$$\mathcal{E}^* = \{S^*, E_1^*, E_2^*, I^*, T^*, R^*\}, \tag{23}$$

where

$$S^* = \frac{\Delta}{\nu \mathbf{R}_0}, \tag{24}$$

$$E_1^* = \frac{1}{\chi_1\chi_4}\left\{\frac{\chi_4\omega\beta}{\mathbf{R}_0} + (1-\rho)\gamma\delta\right\} I^*, \tag{25}$$

$$E_2^* = \frac{1}{\varsigma_2\chi_4}\left(\chi_3\chi_4 - \gamma\delta\rho\right) I^*, \tag{26}$$

$$I^* = \frac{\chi_1\chi_4\nu\varsigma_2(\mathbf{R}_0 - 1)\Delta}{\nu\left\{\begin{array}{c}\chi_4\nu\varsigma_2\beta\omega + (\nu(\chi_1(\chi_3\chi_4 - \delta\gamma\rho)\\ +\gamma\varsigma_2(\chi_1 + (1-\rho)\delta))\\ +\chi_1\varsigma_2(\gamma\phi + \chi_4\nu))\mathbf{R}_0\end{array}\right\}}, \tag{27}$$

$$T^* = \frac{\gamma}{\chi_4} I^*, \tag{28}$$

$$R^* = \frac{\gamma\phi}{\chi_4\nu} I^*. \tag{29}$$

4.1. Basic reproduction number

To determine the basic reproduction number, the next-generation matrix method is employed. The infected compartments are chosen as

$$X = (E_1, E_2, I, T)^T. \tag{30}$$

The vector of newly generated infection terms is given by

$$\mathbb{F}(X) = \begin{pmatrix} \omega\beta I \\ (1-\omega)\beta I \\ 0 \\ 0 \end{pmatrix}, \tag{31}$$

while the remaining transition terms are

$$\mathbb{V}(X) = \begin{pmatrix} \chi_1 E_1 - (1-\rho)\delta T \\ \chi_2 E_2 - \varsigma_1 E_1 \\ \chi_3 I - \varsigma_2 E_2 - \rho\delta T \\ \chi_4 T - \gamma I \end{pmatrix}. \tag{32}$$

Evaluating the Jacobian matrices of $\mathbb{F}$ and $\mathbb{V}$ at the disease-free equilibrium E_0 yields

$$\mathbb{F} = \begin{pmatrix} 0 & 0 & \beta\omega & 0 \\ 0 & 0 & \beta(1-\omega) & 0 \\ 0 & 0 & 0 & 0 \\ 0 & 0 & 0 & 0 \end{pmatrix}, \tag{33}$$

and

$$\mathbb{V} = \begin{pmatrix} \chi_1 & 0 & 0 & -(1-\rho)\delta \\ -\varsigma_1 & \chi_2 & 0 & 0 \\ 0 & -\varsigma_2 & \chi_3 & -\rho\delta \\ 0 & 0 & -\gamma & \chi_4 \end{pmatrix}. \tag{34}$$

The next-generation matrix is therefore

$$K = \mathbb{F}\mathbb{V}^{-1}. \tag{35}$$

Multiplying $\mathbb{F}$ by $\mathbb{V}^{-1}$ and simplifying gives the dominant eigenvalue of K as

$$\rho(K) = \frac{\beta\omega\varsigma_1\varsigma_2}{\chi_1\chi_2\chi_3} + \frac{\beta(1-\omega)\varsigma_2}{\chi_2\chi_3} + \frac{\delta\gamma\varsigma_1\varsigma_2(1-\rho)}{\chi_1\chi_2\chi_3\chi_4} + \frac{\gamma\rho\delta}{\chi_3\chi_4}. \tag{36}$$

Hence, the basic reproduction number is obtained as

$$\mathbf{R}_0 = \frac{\beta\omega\varsigma_1\varsigma_2}{\chi_1\chi_2\chi_3} + \frac{\beta(1-\omega)\varsigma_2}{\chi_2\chi_3} + \frac{\delta\gamma\varsigma_1\varsigma_2(1-\rho)}{\chi_1\chi_2\chi_3\chi_4} + \frac{\gamma\rho\delta}{\chi_3\chi_4}, \tag{37}$$

No additional threshold condition is required for this definition of $\mathbf{R}_0$.

Remark 1. The last two terms in $\mathbf{R}_0$ do not contain β because they arise from the inverse of the transition matrix $\mathbb{V}^{-1}$ (specifically, from treatment failure pathways $T \to E_1$ and $T \to I$), not from the new infection matrix $\mathbb{F}$. This is consistent with the standard NGM construction where $\mathbb{V}^{-1}$ accounts for all transitions between infected compartments before new infections are counted. These terms represent secondary transmission due to relapse or incomplete treatment, which contribute to the overall reproductive capacity of the disease.

Thus, the endemic equilibrium ($\mathcal{E}^*$) exists when $\mathbf{R}_0 > 1$ and is given by (23).

4.2. Sensitivity evaluation

The sensitivity of $\mathbf{R}_0$ may be examined by considering the partial derivatives of $\mathbf{R}_0$ with respect to the relevant parameters. To account explicitly for the parameter dependencies in Eq. (5), write the four contributions to $\mathbf{R}_0$ as $\mathcal{R}_1 = \frac{\beta\omega\varsigma_1\varsigma_2}{\chi_1\chi_2\chi_3}$, $\mathcal{R}_2 = \frac{\beta(1-\omega)\varsigma_2}{\chi_2\chi_3}$, $\mathcal{R}_3 = \frac{\delta\gamma\varsigma_1\varsigma_2(1-\rho)}{\chi_1\chi_2\chi_3\chi_4}$, and $\mathcal{R}_4 = \frac{\gamma\rho\delta}{\chi_3\chi_4}$, so that $\mathbf{R}_0 = \mathcal{R}_1 + \mathcal{R}_2 + \mathcal{R}_3 + \mathcal{R}_4$.

$$\frac{\partial \mathbf{R}_0}{\partial \beta} = \frac{\mathcal{R}_1 + \mathcal{R}_2}{\beta}. \tag{38}$$

$$\frac{\partial \mathbf{R}_0}{\partial \omega} = \frac{\mathcal{R}_1}{\omega} - \frac{\mathcal{R}_2}{1-\omega}. \tag{39}$$

$$\frac{\partial \mathbf{R}_0}{\partial \varsigma_1} = (\mathcal{R}_1 + \mathcal{R}_3)\left(\frac{1}{\varsigma_1} - \frac{1}{\chi_1}\right). \tag{40}$$

$$\frac{\partial \mathbf{R}_0}{\partial \varsigma_2} = (\mathcal{R}_1 + \mathcal{R}_2 + \mathcal{R}_3)\left(\frac{1}{\varsigma_2} - \frac{1}{\chi_2}\right). \tag{41}$$

$$\frac{\partial \mathbf{R}_0}{\partial \gamma} = \frac{\mathcal{R}_3 + \mathcal{R}_4}{\gamma} - \frac{\mathbf{R}_0}{\chi_3}. \tag{42}$$

$$\frac{\partial \mathbf{R}_0}{\partial \rho} = -\frac{\mathcal{R}_3}{1-\rho} + \frac{\mathcal{R}_4}{\rho}. \tag{43}$$

$$\frac{\partial \mathbf{R}_0}{\partial \delta} = (\mathcal{R}_3 + \mathcal{R}_4)\left(\frac{1}{\delta} - \frac{1}{\chi_4}\right). \tag{44}$$

$$\frac{\partial \mathbf{R}_0}{\partial \sigma_1} = -\frac{\mathbf{R}_0}{\chi_3}. \tag{45}$$

$$\frac{\partial \mathbf{R}_0}{\partial \sigma_2} = -\frac{\mathcal{R}_3 + \mathcal{R}_4}{\chi_4}. \tag{46}$$

$$\frac{\partial \mathbf{R}_0}{\partial \phi} = -\frac{\mathcal{R}_3 + \mathcal{R}_4}{\chi_4}. \tag{47}$$

$$\begin{aligned}\frac{\partial \mathbf{R}_0}{\partial \nu} = &-\mathcal{R}_1\left(\frac{1}{\chi_1} + \frac{1}{\chi_2} + \frac{1}{\chi_3}\right)\\ &-\mathcal{R}_2\left(\frac{1}{\chi_2} + \frac{1}{\chi_3}\right)\\ &-\mathcal{R}_3\left(\frac{1}{\chi_1} + \frac{1}{\chi_2} + \frac{1}{\chi_3} + \frac{1}{\chi_4}\right)\\ &-\mathcal{R}_4\left(\frac{1}{\chi_3} + \frac{1}{\chi_4}\right).\end{aligned} \tag{48}$$

The normalized forward sensitivity index of the basic reproduction number $\mathbf{R}_0$ with respect to a parameter p is defined as

$$\Gamma_p^{\mathbf{R}_0} = \frac{\partial \mathbf{R}_0}{\partial p} \times \frac{p}{\mathbf{R}_0}, \tag{49}$$

which measures the relative change in $\mathbf{R}_0$ due to a relative change in the parameter p. A positive (negative) index indicates that an increase in p leads to an increase/decrease in $\mathbf{R}_0$. The normalized indices are reported in Table 2, and their graphical representation is shown in Figure 1.

The sensitivity analysis reveals:

- The transmission coefficient β ($\Gamma_\beta^{\mathbf{R}_0} = +0.9186$) is the most influential positive parameter, indicating that reducing contact rates is an important control strategy.

Table 2: Normalized forward sensitivity indices of $\mathbf{R}_0$ with respect to model parameters.

Parameter	$\Gamma_p^{\mathbf{R}_0}$	Interpretation
β	+0.9186	Strong positive; most influential parameter
ω	−0.0254	Weak negative; increasing ω slightly reduces $\mathbf{R}_0$
ς_1	+0.0269	Weak positive influence
ς_2	+0.1252	Weak positive influence
δ	+0.0535	Weak positive influence
γ	−0.2607	Moderate negative influence
ρ	+0.0048	Negligible positive influence
σ_1	−0.6243	Moderate negative influence
σ_2	−0.0429	Weak negative influence
ϕ	−0.0043	Negligible negative influence
ν	−0.1921	Weak negative influence

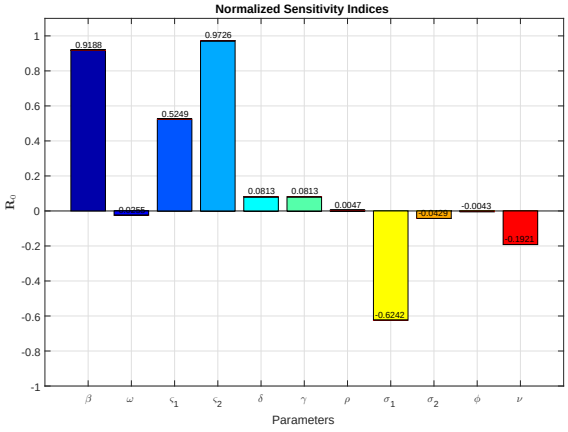

Figure 1: Sensitivity analysis of the model parameters.

- The disease-induced death rate σ_1 ($\Gamma_{\sigma_1}^{\mathbf{R}_0} = -0.6243$) has the strongest negative sensitivity, while the treatment rate γ ($\Gamma_\gamma^{\mathbf{R}_0} = -0.2607$) has a moderate negative sensitivity.
- The remaining parameters, including ω, ς_1, ς_2, δ, ρ, σ_2, ϕ, and ν, have smaller absolute sensitivity indices for the parameter values used in this study.

4.3. Existence and uniqueness

This section focuses at the suggested equational framework for fractional calculus survival, including its novelty and use. The following theorem needs to be established in order to achieve this.

Theorem 4.1. Suppose that there are positive constants, λ_j and its $\overline{\lambda}_j$, so that

$$i.\quad |H_j(x_j,t)-H_j(x_j^{'},t)|\le \lambda_j|x_j-x_j^{'}|,\quad \forall j\in\{1,2,\cdots,6\}. \tag{50}$$

$$ii.\quad |H_j(x_j,t)|^2\le \overline{\lambda_j}(1+|x_j|),\quad \forall (x,t)\in R^6\times[0,T]. \tag{51}$$

Proof. Remembering our model now

$$\begin{cases} {}^{ABC}\mathbb{D}_t^{\tau}S(t)=\Delta-\frac{\beta S I}{N}-\nu S & =H_1(t,\Upsilon),\\ {}^{ABC}\mathbb{D}_t^{\tau}E_1(t)=\omega\frac{\beta S I}{N}-\chi_1E_1+(1-\rho)\delta T & =H_2(t,\Upsilon),\\ {}^{ABC}\mathbb{D}_t^{\tau}E_2(t)=(1-\omega)\frac{\beta S I}{N}+\varsigma_1E_1-\chi_2E_2 & =H_3(t,\Upsilon),\\ {}^{ABC}\mathbb{D}_t^{\tau}I(t)=\varsigma_2E_2+\rho\delta T-\chi_3I & =H_4(t,\Upsilon),\\ {}^{ABC}\mathbb{D}_t^{\tau}T(t)=\gamma I-\chi_4T & =H_5(t,\Upsilon),\\ {}^{ABC}\mathbb{D}_t^{\tau}R(t)=\phi T-\nu R & =H_6(t,\Upsilon), \end{cases} \tag{52}$$

where $\Upsilon=\{S,E_1,E_2,I,T,R\}$.

The function $H_1(t,\Upsilon)$ is where we begin. Next, we'll demonstrate that

$$\left|H_1(S^1,t)-H_1(S^2,t)\right|^2\le\lambda_1\left|S^1-S^2\right|^2. \tag{53}$$

Then, we write

$$\begin{aligned} \left|H_1(S^1,t)-H_1(S^2,t)\right|^2&=\left|-\frac{\beta I(S^1-S^2)}{N}-\nu(S^1-S^2)\right|^2,\\ \left|H_1(S^1,t)-H_1(S^2,t)\right|^2&=\left|-\left\{\frac{\beta I}{N}+\nu\right\}(S^1-S^2)\right|^2,\\ \left|H_1(S^1,t)-H_1(S^2,t)\right|^2&=\left|\left\{\frac{\beta I}{N}+\nu\right\}(S^1-S^2)\right|^2,\\ \left|H_1(S^1,t)-H_1(S^2,t)\right|^2&\le\left\{2\frac{\beta^2|I|^2}{N^2}+2\nu^2\right\}\left|(S^1-S^2)\right|^2,\\ &\le\left\{2\frac{\beta^2\sup_{0\le t\le T}|I|^2}{N^2}+2\nu^2\right\}\left|(S^1-S^2)\right|^2,\\ \left|H_1(S^1,t)-H_1(S^2,t)\right|^2&\le\left\{2\frac{\beta^2|I|_\infty^2}{N^2}+2\nu^2\right\}\left|(S^1-S^2)\right|^2,\\ \left|H_1(S^1,t)-H_1(S^2,t)\right|^2&\le\lambda_1\left|(S^1-S^2)\right|^2,\\ \lambda_1&=\left\{2\frac{\beta^2|I|_\infty^2}{N^2}+2\nu^2\right\}. \end{aligned} \tag{54}$$

Similarly, we solve for other then we get

$$\begin{aligned} &\lambda_2=\chi_1^2,\ \ \lambda_3=\chi_2^2,\ \ \lambda_4=\chi_3^2,\\ &\lambda_5=\chi_4^2,\ \ \lambda_6=\nu^2. \end{aligned} \tag{55}$$

For every function, we performed two starting condition tests. We have now verified the second condition of our model.

$$|H_1(S,t)|^2=\left|\Delta-\frac{S\beta I}{N}-S\nu\right|^2, \tag{56}$$

$$|H_1(S,t)|^2=\left|\Delta-\left\{\frac{\beta I}{N}+\nu\right\}S\right|^2, \tag{57}$$

$$|H_1(S,t)|^2\le\Delta^2 2+2\left\{\frac{\beta|I|}{N}+\nu\right\}^2|S|^2, \tag{58}$$

$$|H_1(S,t)|^2\le\Delta^2 2+\left\{\frac{\sup_{0\le t\le T}|I|\beta}{N}+\nu\right\}^2 2|S|^2, \tag{59}$$

$$|H_1(S,t)|^2\le\Delta^2 2+2\left\{\frac{\beta|I|_\infty}{N}+\nu\right\}^2|S|^2, \tag{60}$$

$$|H_1(S,t)|^2\le 2\Delta^2\left[1+\frac{\left\{\frac{\beta|I|_\infty}{N}+\nu\right\}^2}{\Delta^2}|S|^2\right], \tag{61}$$

$$|H_1(S_1,t)|^2\le\overline{\lambda}_1\left(1+|S|^2\right), \tag{62}$$

under the condition $\left\{\frac{\left\{\frac{\beta|I|_\infty}{N}+\nu\right\}^2}{\Delta^2}\right\}<1$,

$$|H_2(E_1,t)|^2=\left|\omega\frac{\beta S I}{N}-\chi_1E_1+(1-\rho)\delta T\right|^2, \tag{63}$$

$$|H_2(E_1,t)|^2=\left|\omega\frac{\beta S I}{N}+(1-\rho)\delta T-\chi_1E_1\right|^2, \tag{64}$$

$$|H_2(E_1,t)|^2\le 2\omega^2\frac{\beta^2|S|^2|I|^2}{N^2}+2(1-\rho)^2\delta^2|T|^2+2\chi_1^2|E_1|^2, \tag{65}$$

$$|H_2(E_1,t)|^2\le 2\omega^2\frac{\beta^2\sup_{0\le t\le T}|S|^2\sup_{0\le t\le T}|I|^2}{N^2}+2(1-\rho)^2\delta^2\sup_{0\le t\le T}|T|^2+2\chi_1^2|E_1|^2. \tag{66}$$

$$|H_2(E_1,t)|^2\le\omega^2 2\frac{\beta^2|S|_\infty^2|I|_\infty^2}{N^2}+2(1-\rho)^2\delta^2|T|_\infty{}^2+2\chi_1^2|E_1|^2 \tag{67}$$

$$|H_2(E_1,t)|^2\le 2\left\{\omega^2\frac{\beta^2|S|_\infty^2|I|_\infty^2}{N^2}+(1-\rho)^2\delta^2|T|_\infty{}^2\right\}\times\left[1+\frac{\chi_1^2}{\frac{\beta^2|S|_\infty^2|I|_\infty^2\omega^2}{N^2}+(1-\rho)^2\delta^2|T|_\infty{}^2}|E_1|^2\right]. \tag{68}$$

$$|H_2(E_1,t)|^2\le\overline{\lambda}_2\left(1+|E_1|^2\right), \tag{69}$$

under the condition $\left\{\frac{\chi_1^2}{\omega^2\frac{\beta^2|S|_\infty^2|I|_\infty^2}{N^2}+(1-\rho)^2\delta^2|T|_\infty{}^2}\right\}<1$,

$$|H_3(E_2,t)|^2=\left|(-\omega+1)\frac{\beta S I}{N}+\varsigma_1E_1-\chi_2E_2\right|^2, \tag{70}$$

$$|H_3(E_2,t)|^2\le(-\omega+1)^2 2\frac{\beta^2|S|^2|I|^2}{N^2}+2\varsigma_1^2|E_1|^2+2\chi_2^2|E_2|^2, \tag{71}$$

$$|H_3(E_2,t)|^2\le 2(-\omega+1)^2\frac{\beta^2\sup_{0\le t\le T}|S|^2\sup_{0\le t\le T}|I|^2}{N^2}+2\varsigma_1^2\sup_{0\le t\le T}|E_1|^2+2\chi_2^2|E_2|^2, \tag{72}$$

$$|H_3(E_2,t)|^2\le(-\omega+1)^2 2\frac{\beta^2|S|_\infty^2|I|_\infty^2}{N^2}+2\varsigma_1^2|E_1|_\infty^2+2\chi_2^2|E_2|^2, \tag{73}$$

$$|H_3(E_2,t)|^2 \le \left\{(-\omega+1)^2\frac{\beta^2|S|_\infty^2|I|_\infty^2}{N^2} + \varsigma_1^2|E_1|_\infty^2\right\} \times 2\left[1+\frac{\chi_2^2}{(-\omega+1)^2\frac{\beta^2|S|_\infty^2|I|_\infty^2}{N^2}+\varsigma_1^2|E_1|_\infty^2}|E_2|^2\right], \tag{74}$$

$$|H_3(E_2,t)|^2 \le \overline{\lambda}_3\left(1+|E_2|^2\right), \tag{75}$$

under the condition $\left\{\frac{\chi_2^2}{(-\omega+1)^2\frac{\beta^2|S|_\infty^2|I|_\infty^2}{N^2}+\varsigma_1^2|E_1|_\infty^2}\right\} < 1$,

$$|H_4(I,t)|^2 = |\varsigma_2 E_2 + \rho\delta T - \chi_3 I|^2, \tag{76}$$

$$|H_4(I,t)|^2 \le 2\varsigma_2^2|E_2|^2 + 2\rho^2|T|^2\delta^2 + 2\chi_3^2|I|^2, \tag{77}$$

$$|H_4(I,t)|^2 \le 2\varsigma_2^2 \sup_{0\le t\le T}|E_2|^2 + 2\sup_{0\le t\le T}|T|^2\rho^2\delta^2 + 2\chi_3^2|I|^2, \tag{78}$$

$$|H_4(I,t)|^2 \le 2\varsigma_2^2|E_2|_\infty^2 + 2\rho^2|T|_\infty^2\delta^2 + 2\chi_3^2|I|^2, \tag{79}$$

$$|H_4(I,t)|^2 \le 2\left\{\varsigma_2^2|E_2|_\infty^2 + \rho^2\delta^2|T|_\infty^2\right\} \times \left[1+|I|^2\frac{\chi_3^2}{\varsigma_2^2|E_2|_\infty^2+\rho^2\delta^2|T|_\infty^2}\right]. \tag{80}$$

$$|H_4(I,t)|^2 \le \left(1+|I|^2\right)\overline{\lambda}_4, \tag{81}$$

under the condition $\left\{\frac{\chi_3^2}{\varsigma_2^2|E_2|_\infty^2+\rho^2\delta^2|T|_\infty^2}\right\} < 1$,

$$|H_5(T,t)|^2 = |\gamma I - \chi_4 T|^2, \tag{82}$$

$$|H_5(T,t)|^2 \le \gamma^2 2|I|^2 + 2\chi_4^2|T|^2, \tag{83}$$

$$|H_5(T,t)|^2 \le \gamma^2 2\sup_{0\le t\le T}|I|^2 + 2\chi_4^2|T|^2, \tag{84}$$

$$|H_5(T,t)|^2 \le \gamma^2 2|I|_\infty^2 + 2\chi_4^2|T|^2, \tag{85}$$

$$|H_5(T,t)|^2 \le \left\{\gamma^2|I|_\infty^2\right\}2\left[1+\frac{\chi_4^2}{|I|_\infty^2\gamma^2}|T|^2\right], \tag{86}$$

$$|H_5(T,t)|^2 \le \overline{\lambda}_5\left(1+|T|^2\right), \tag{87}$$

under the condition $\left\{\frac{\chi_4^2}{\gamma^2|I|_\infty^2}\right\} < 1$,

$$|H_6(R,t)|^2 = |T\phi - R\nu|^2, \tag{88}$$

$$|H_6(R,t)|^2 \le |T|^2\phi^2 2 + |R|^2\nu^2 2, \tag{89}$$

$$|H_6(R,t)|^2 \le \sup_{0\le t\le T}|T|^2\phi^2 2 + \nu^2 2|R|^2, \tag{90}$$

$$|H_6(R,t)|^2 \le \phi^2|T|_\infty^2 2 + \nu^2 2|R|^2, \tag{91}$$

$$|H_6(R,t)|^2 \le \left\{|T|_\infty^2\phi^2\right\}2\left[1+|R|^2\frac{\nu^2}{|T|_\infty^2\phi^2}\right], \tag{92}$$

$$|H_6(R,t)|^2 \le \left(1+|R|^2\right)\overline{\lambda}_6, \tag{93}$$

under the condition $\left\{\frac{\nu^2}{\phi^2|T|_\infty^2}\right\} < 1$.

As a result, the model admits a unique solution.

$$\max\begin{Bmatrix}\left\{\frac{\left\{\frac{\beta|I|_\infty}{N}+\nu\right\}^2}{\Delta^2}\right\},\\ \left\{\frac{\chi_1^2}{\omega^2\frac{\beta^2|S|_\infty^2|I|_\infty^2}{N^2}+(1-\rho)^2\delta^2|T|_\infty}\right\},\\ \left\{\frac{\chi_2^2}{(1-\omega)^2\frac{\beta^2|S|_\infty^2|I|_\infty^2}{N^2}+\varsigma_1^2|E_1|_\infty^2}\right\},\\ \left\{\frac{\chi_3^2}{\varsigma_2^2|E_2|_\infty^2+\rho^2\delta^2|T|_\infty^2}\right\},\\ \left\{\frac{\chi_4^2}{\gamma^2|I|_\infty^2}\right\},\\ \left\{\frac{\nu^2}{\phi^2|T|_\infty^2}\right\}.\end{Bmatrix} < 1 \tag{94}$$

Condition (94) plays a fundamental role in establishing the existence and uniqueness of solutions. In particular, it guarantees that the nonlinear operator associated with the integral form of the model satisfies the contraction condition. Since the maximum Lipschitz constant of all model components is less than one, the operator becomes a contraction mapping on the chosen Banach space. Therefore, by the Banach Fixed-Point Theorem, the proposed fractional-order tuberculosis model admits a unique solution. □

4.4. Stability analysis

A qualitative examination of the suggested model system (4) is carried out in order to gain understanding of its dynamical features. The impact of control measures on the dynamics of the proposed transmission of the tuberculosis illness is better understood due to this investigation.

4.5. Local stability

Theorem 4.2. The disease-free equilibrium ($\mathcal{E}^0$) is locally asymptotically stable if the eigenvalues λ_j of the suggested model (4) satisfy $|\arg(\lambda_j)| > \frac{\tau\pi}{2}$ for $\tau \in (0,1]$.

Proof. The Jacobian matrix at $\mathcal{E}^0$ for the system (4) is

$$\mathbb{J}(E_0) = \begin{bmatrix} -\nu & 0 & 0 & -\beta & 0 & 0\\ 0 & -\chi_1 & 0 & \omega\beta & (1-\rho)\delta & 0\\ 0 & \varsigma_1 & -\chi_2 & \beta(1-\omega) & 0 & 0\\ 0 & 0 & \varsigma_2 & -\chi_3 & \delta\rho & 0\\ 0 & 0 & 0 & \gamma & -\chi_4 & 0\\ 0 & 0 & 0 & 0 & \phi & -\nu \end{bmatrix}, \tag{95}$$

where $\chi_1 = \nu+\varsigma_1, \chi_2 = \nu+\varsigma_2, \chi_3 = \nu+\gamma+\sigma_1$, and $\chi_4 = \nu+\delta+\sigma_2+\phi$. The characteristic polynomial $P(\lambda) = \det(\lambda I - \mathbb{J}(\mathcal{E}^0))$ gives two eigenvalues

$$\lambda_1 = \lambda_2 = -\nu < 0. \tag{96}$$

The remaining eigenvalues satisfy the equation:

$$P(\lambda) = \lambda^4 + b_1\lambda^3 + b_2\lambda^2 + b_3\lambda + b_4, \tag{97}$$

where

$$\begin{aligned} b_1 &= \chi_1 + \chi_2 + \chi_3 + \chi_4, \\ b_2 &= \chi_1\chi_2 + \chi_1\chi_3 + \chi_1\chi_4 + \chi_2\chi_3 + \chi_2\chi_4 + \chi_3\chi_4 \\ &\quad - \beta\omega\varsigma_1 - \beta(1-\omega)\chi_1 - \delta\gamma\rho\chi_1, \\ b_3 &= \chi_1\chi_2\chi_3 + \chi_1\chi_2\chi_4 + \chi_1\chi_3\chi_4 + \chi_2\chi_3\chi_4 \\ &\quad - \beta\omega\varsigma_1(\chi_2+\chi_4) - \beta(1-\omega)\chi_1(\chi_3+\chi_4) \\ &\quad - \delta\gamma\rho\chi_1(\chi_1+\chi_2) - \delta\gamma\varsigma_1\varsigma_2(1-\rho), \\ b_4 &= \chi_1\chi_2\chi_3\chi_4(1-\mathbf{R}_0). \end{aligned} \tag{98}$$

Substituting the expressions for $\chi_1, \chi_2, \chi_3, \chi_4$ and $\mathbf{R}_0$, it can be verified that:

- $b_1 > 0$ since all $\chi_i > 0$.
- $b_2 > 0$ because the positive terms dominate the negative terms when $\mathbf{R}_0 < 1$.
- $b_3 > 0$ under the condition $\mathbf{R}_0 < 1$.
- $b_4 > 0$ if and only if $\mathbf{R}_0 < 1$.
- $b_1 b_2 - b_3 > 0$ and $b_1 b_2 b_3 - b_1^2 b_4 - b_3^2 > 0$ follow directly from the positivity of parameters and the condition $\mathbf{R}_0 < 1$.

Thus, all Routh-Hurwitz conditions are satisfied, implying that all roots of $P(\lambda)$ have negative real parts, i.e., $\Re(\lambda_i) < 0$ for $i = 1, 2, 3, 4$. For the fractional-order system of order $\tau \in (0, 1]$, Matignon's stability criterion yields

$$|\arg(\lambda_i)| > \frac{\tau\pi}{2}, \tag{99}$$

thereby establishing the local asymptotic stability of the disease-free equilibrium $\mathcal{E}^0$ whenever $\mathbf{R}_0 < 1$. □

4.6. Global stability

We will show that the proposed demonstration is Lyapunov stable in this section. We set the model independent variables to $\{S, E_1, E_2, I, T, R\}$ and ${}^{ABC}\mathbb{D}_t^\tau L < 0$, which in our case indicates the unfavourable equilibrium E^*, for the endemic Lyapunov function.

Theorem 4.3. Assume $\mathbf{R}_0 > 1$ so that the endemic equilibrium E^* exists. If $\psi \le \varpi$ for all states in Γ, with equality only at E^*, then E^* is globally asymptotically stable in Γ.

Proof. The Lyapunov function can be expressed as follows

$$\begin{aligned} L(S^*, E_1^*, E_2^*, I^*, T^*, R^*) &= (S - S^* - S^* \log \frac{S^*}{S}) \\ &\quad + (E_1 - E_1^* - E_1^* \log \frac{E_1^*}{E_1}) \\ &\quad + (E_2 - E_2^* - E_2^* \log \frac{E_2^*}{E_2}) \\ &\quad + (I - I^* - I^* \log \frac{I^*}{I}) \\ &\quad + (T - T^* - T^* \log \frac{T^*}{T}) \\ &\quad + (R - R^* - R^* \log \frac{R^*}{R}). \end{aligned} \tag{100}$$

It is therefore wise to use the derivative with respect to t.

$$\begin{aligned} {}^{ABC}\mathbb{D}_t^\tau L \le{}& (\frac{S - S^*}{S})^{ABC}\mathbb{D}_t^\tau S + (\frac{E_1 - E_1^*}{E_1})^{ABC}\mathbb{D}_t^\tau E_1 \\ &+ (\frac{E_2 - E_2^*}{E_2})^{ABC}\mathbb{D}_t^\tau E_2 + (\frac{I - I^*}{I})^{ABC}\mathbb{D}_t^\tau I \\ &+ (\frac{T - T^*}{T})^{ABC}\mathbb{D}_t^\tau T + (\frac{R - R^*}{R})^{ABC}\mathbb{D}_t^\tau R. \end{aligned} \tag{101}$$

The values of their derivatives can now be written as follows.

$$\begin{aligned} {}^{ABC}\mathbb{D}_t^\tau L \le{}& (\frac{S - S^*}{S})(\Delta - \frac{\beta S I}{N} - \nu S) \\ &+ (\frac{E_1 - E_1^*}{E_1})(\omega\frac{\beta S I}{N} - \chi_1 E_1 + (1-\rho)\delta T) \\ &+ (\frac{E_2 - E_2^*}{E_2})((1-\omega)\frac{\beta S I}{N} + \varsigma_1 E_1 - \chi_2 E_2) \\ &+ (\frac{I - I^*}{I})(\varsigma_2 E_2 + \rho\delta T - \chi_3 I) \\ &+ (\frac{T - T^*}{T})(\gamma I - \chi_4 T) \\ &+ (\frac{R - R^*}{R})(\phi T - \nu R). \end{aligned} \tag{102}$$

Putting $S = S - S^*$, $E_1 = E_1 - E_1^*$, $E_2 = E_2 - E_2^*$, $I = I - I^*$, $T = T - T^*$ and $R = R - R^*$ leads to

$$\begin{aligned} {}^{ABC}\mathbb{D}_t^\tau L \le{}& ((\frac{S - S^*}{S})(\Delta - \frac{\beta(S - S^*)(I - I^*)}{N} - \nu(S - S^*)) \\ &+ (\frac{E_1 - E_1^*}{E_1})(\omega\frac{\beta(S - S^*)(I - I^*)}{N} - \chi_1(E_1 - E_1^*) \\ &+ (1-\rho)\delta(T - T^*)) + (\frac{E_2 - E_2^*}{E_2}) \\ &((1-\omega)\frac{\beta(S - S^*)(I - I^*)}{N} + \varsigma_1(E_1 - E_1^*) \\ &- \chi_2(E_2 - E_2^*)) + (\frac{I - I^*}{I})(\varsigma_2(E_2 - E_2^*) \\ &+ \rho\delta(T - T^*) - \chi_3(I - I^*)) + (\frac{T - T^*}{T})(\gamma(I - I^*) \\ &- \chi_4(T - T^*)) + (\frac{R - R^*}{R})(\phi(T - T^*) - \nu(R - R^*)). \end{aligned} \tag{103}$$

The above can be expressed simply as

$${}^{ABC}\mathbb{D}_t^\tau L \le \psi - \varpi, \tag{104}$$

where

$$\begin{aligned}\psi = \Delta &+ \frac{\beta I^*}{N}\frac{(S-S^*)^2}{S} + \frac{\omega S I}{N} + \frac{\omega S^* I^*}{N} \\ &+ \frac{\omega S I^*}{N}\frac{E_1^*}{E_1} + \frac{\omega S^* I}{N}\frac{E_1^*}{E_1} + \delta T + \delta\rho T^* \\ &+ \delta T^*\frac{E_1^*}{E_1} + \delta\rho T\frac{E_1^*}{E_1} + \frac{\beta S I}{N} + \frac{\beta S^* I^*}{N} \\ &+ \omega\frac{\beta S I^*}{N} + \omega\frac{\beta S^* I}{N} + \frac{\beta S I^*}{N}\frac{E_2^*}{E_2} \\ &+ \frac{\beta S^* I}{N}\frac{E_2^*}{E_2} + \omega\frac{\beta S I}{N}\frac{E_2^*}{E_2} \\ &+ \omega\frac{\beta S^* I^*}{N}\frac{E_2^*}{E_2} + \varsigma_1 E_1 + \varsigma_1 E_1^*\frac{E_2^*}{E_2} \\ &+ \varsigma_2 E_2 + \rho\delta T + \varsigma_2 E_2^*\frac{I^*}{I} \\ &+ \rho\delta T^*\frac{I^*}{I} + \gamma I + \gamma I^*\frac{T^*}{T} \\ &+ \phi T + \phi T^*\frac{R^*}{R},\end{aligned} \tag{105}$$

and

$$\begin{aligned}\varpi = \Delta\frac{S^*}{S} &+ \frac{\beta I}{N}\frac{(S-S^*)^2}{S} + \frac{\omega S I^*}{N} \\ &+ \frac{\omega S^* I}{N} + \frac{\omega S I}{N}\frac{E_1^*}{E_1} + \frac{\omega S^* I^*}{N}\frac{E_1^*}{E_1} \\ &+ \chi_1\frac{(E_1-E_1^*)^2}{E_1} + \delta T^* + \delta\rho T \\ &+ \delta T\frac{E_1^*}{E_1} + \delta\rho T^*\frac{E_1^*}{E_1} + \frac{\beta S I^*}{N} \\ &+ \frac{\beta S^* I}{N} + \omega\frac{\beta S I}{N} + \omega\frac{\beta S^* I^*}{N} \\ &+ \frac{\beta S I}{N}\frac{E_2^*}{E_2} + \frac{\beta S^* I^*}{N}\frac{E_2^*}{E_2} \\ &+ \omega\frac{\beta S I^*}{N}\frac{E_2^*}{E_2} + \omega\frac{\beta S^* I}{N}\frac{E_2^*}{E_2} \\ &+ \varsigma_1 E_1^* + \varsigma_1 E_1\frac{E_2^*}{E_2} + \chi_2\frac{(E_2-E_2^*)^2}{E_2} \\ &+ \varsigma_2 E_2^* - \rho\delta T^* + \varsigma_2 E_2\frac{I^*}{I} \\ &+ \rho\delta T\frac{I^*}{I} + \frac{(I-I^*)^2\chi_3}{I} \\ &+ \gamma I^* + \gamma I\frac{T^*}{T} + \frac{(T-T^*)^2\chi_4}{T} \\ &+ \phi T^* - \frac{T\phi R^*}{R} + \frac{(R-R^*)^2\nu}{R}.\end{aligned} \tag{106}$$

It has been concluded that if $\psi < \varpi$, this yields ${}^{ABC}\mathbb{D}_t^\tau L < 0$, when, however $S = S^*$, $E_1 = E_1^*$, $E_2 = E_2^*$, $I = I^*$, $T = T^*$, and $R = R^*$ is

$$0 = \psi - \varpi \Rightarrow {}^{ABC}\mathbb{D}_t^\tau L \leq 0 \tag{107}$$

It is evident that the suggested model has the largest invariant compact set in

$$\{(S^*, E_1^*, E_2^*, I^*, T^*, R^*) \in \Gamma : {}^{ABC}\ \mathbb{D}_t^\tau L = 0\}. \tag{108}$$

According to LaSalle's invariance principle, the global-stability conclusion requires $\psi \leq \varpi$ throughout Γ and equality only at E^*.

For the global-stability argument, the inequality $\psi \leq \varpi$ throughout Γ is imposed as an additional sufficient condition. The quantities ψ and ϖ are explicitly defined as the positive and negative contributions appearing in the Atangana–Baleanu–Caputo derivative of the Lyapunov function, respectively, where

$$\psi = \sum_{i=1}^{n} P_i(S, E_1, E_2, I, T, R), \tag{109}$$

denotes the collection of nonnegative terms arising from the transmission, progression, and treatment dynamics, while

$$\varpi = \sum_{j=1}^{m} Q_j(S, E_1, E_2, I, T, R), \tag{110}$$

represents the dissipative terms associated with natural mortality, disease-induced mortality, treatment removal, and recovery processes.

To examine this sufficient condition, we use the endemic equilibrium relations from system (4) at E^*, where all fractional derivatives vanish. These relations provide the following identities:

$$\begin{aligned}\Delta &= \frac{\beta S^* I^*}{N} + \nu S^*, \\ \chi_1 E_1^* &= \omega\frac{\beta S^* I^*}{N} + (1-\rho)\delta T^*, \\ \chi_2 E_2^* &= (1-\omega)\frac{\beta S^* I^*}{N} + \varsigma_1 E_1^*, \\ \chi_3 I^* &= \varsigma_2 E_2^* + \rho\delta T^*, \\ \chi_4 T^* &= \gamma I^*, \\ \nu R^* &= \phi T^*.\end{aligned} \tag{111}$$

If the required termwise estimates are satisfied, substituting these equilibrium relations into (103) gives the desired nonpositive form

$${}^{ABC}\mathbb{D}_t^\tau L \leq -\sum_k \alpha_k\left(\frac{x_k - x_k^*}{x_k}\right)^2 \leq 0, \tag{112}$$

where $\alpha_k > 0$ are combinations of model parameters and $x_k \in \{S, E_1, E_2, I, T, R\}$. Each squared term is nonnegative, ensuring that ${}^{ABC}\mathbb{D}_t^\tau L \leq 0$.

However, a fully rigorous verification of the termwise inequality $P_i \leq k_i Q_i$ with $0 < k_i < 1$ for all admissible solutions in Γ requires extensive algebraic manipulation and is beyond the scope of this proof. Therefore, we present the global stability result as follows:

Remark 2. The endemic equilibrium E^* of system (4) is globally asymptotically stable in the feasible region Γ provided that

$$\psi \leq \varpi \quad \text{for all } (S, E_1, E_2, I, T, R) \in \Gamma, \tag{113}$$

with equality only at E^*; under this condition ${}^{ABC}\mathbb{D}_t^\tau L \leq 0$. This is an additional sufficient condition for the stated global-stability result.

A sufficient termwise condition is

$$P_i(S, E_1, E_2, I, T, R) \le k_i\, Q_i(S, E_1, E_2, I, T, R), \qquad 0 < k_i < 1, \tag{114}$$

for all admissible solutions in Γ. Consequently,

$$\psi \le k\varpi, \qquad 0 < k < 1. \tag{115}$$

Therefore,

$${}^{ABC}D_t^{\tau} L \le \psi - \varpi \le (k-1)\varpi \le 0. \tag{116}$$

The equality holds only when

$$S = S^*, \quad E_1 = E_1^*, \quad E_2 = E_2^*, \quad I = I^*, \quad T = T^*, \quad R = R^*. \tag{117}$$

Hence, the Lyapunov function is positive definite and its Atangana–Baleanu–Caputo fractional derivative is negative semi-definite throughout the positively invariant region Γ. Therefore, by the fractional Lyapunov direct method together with LaSalle's invariance principle, the endemic equilibrium point E^* is globally asymptotically stable whenever $\mathbf{R}_0 > 1$ and the inequality $\psi \le \varpi$ is satisfied throughout Γ, with equality only at E^*. □

4.7. Analysis of the suggested model

With the help of approaching fixed point theorem existing result of considered model is highlighted in this section of paper. Is solution required or not this information is provided by fixed point theory. This theory is a check of existence of modeling physical phenomena. Now we select the Banach space $\Theta = C([0,T], R)$ according to norm $\|Z\| = \sup_{t\in[0,T]} |Z(t)|$. Now we show the BS $F = (\Theta^6, \| \ Z \ \|)$ with norm

$$\|Z\| = \sup_{t\in[0,T]} \left(|S(t)| + |E_2(t)| + |E_1(t)| + |I(t)| + |T(t)| + |R(t)|\right), \tag{118}$$

to get the model's predictions as results

$$\begin{cases} G_1(t,S,E_1,E_2,I,T,R) = \Delta - \frac{\beta S I}{N} - \nu S, \\ G_2(t,S,E_1,E_2,I,T,R) = \omega\frac{\beta S I}{N} - \chi_1 E_1 + (1-\rho)\delta T, \\ G_3(t,S,E_1,E_2,I,T,R) = (1-\omega)\frac{\beta S I}{N} + \varsigma_1 E_1 - \chi_2 E_2, \\ G_4(t,S,E_1,E_2,I,T,R) = \varsigma_2 E_2 + \rho\delta T - \chi_3 I, \\ G_5(t,S,E_1,E_2,I,T,R) = \gamma I - \chi_4 T, \\ G_6(t,S,E_1,E_2,I,T,R) = \phi T - \nu R. \end{cases} \tag{119}$$

Next, the model (4)-(6) can be described this way

$$\begin{cases} {}^{ABC}\mathbb{D}_t^{\tau} Z(t) = & \Psi(t, Z(t)) \\ Z(0) = & Z_0 \end{cases} \tag{120}$$

where

$$\begin{cases} Z(t) = (S, E_1, E_2, I, T, R)^T, \\ Z(0) = (S(0), E_1(0), E_2(0), I(0), T(0), R(0))^T, \\ \Psi(t, Z(t)) = G_i(t, E_1, E_2, I, T, R)^T; \quad i = 1, 2, 3, \cdots, 6. \end{cases} \tag{121}$$

a vector's transpose is defined as $(.)^T$. Problem (120) is equivalent to the subsequent non-integer IE.

$$Z(t) = Z_0 + \frac{1-\tau}{Z(\tau)}\Psi(t, Z(t)) + \frac{\tau}{Z(\tau)\Gamma(\tau)}\int_0^t (t-\eta)^{\tau-1}\Psi(\eta, Z(\eta))d\eta. \tag{122}$$

Schauder's fixed-point theorem can avail the existence results for the proposed model (4)-(6) are generate.

Theorem 4.4. Now consider a continuous function is $\Psi \in \mathbb{F}$ and exist a constant $M > 0, \ni |\Psi(t, Z(t))| \le M(1 + |Z|), \forall t \in [0, T]$ and $Z \in \mathbb{F}$. We got one solution (at-least) for suggested model as (5)-(4).

$$\Delta_1 = \frac{MT^{\tau} + (1-\tau)\Gamma(\tau)M}{Z(\tau)\Gamma(\tau)} < 1. \tag{123}$$

Proof. The operator is $y : \mathbb{F} \to \mathbb{F}$,

$$\begin{aligned} Y(Z)(t) = Z_0 + \frac{-\tau+1}{Z(\tau)}\Psi(t, Z(t)) \\ + \frac{\tau}{Z(\tau)\Gamma(\tau)}\int_0^t (t-\eta)^{\tau-1}\Psi(\eta, Z(\eta))d\eta. \end{aligned} \tag{124}$$

We want to show the closed, convex and bounded ball as $B_{\varpi} = \{Z \in \Psi : \|Z \le \varpi, \varpi > 0\|\}$ with $\varpi \ge \frac{\Delta_2}{1-\Delta_1}$,

$$\Delta_2 = |Z_0| + \frac{-\tau+1}{Z(\tau)}M + \frac{T^{\tau}}{Z(\tau)\Gamma(\tau)}M. \tag{125}$$

Let we demonstrated it $(YB_{\varpi}) \subset B_{\varpi}, \forall t \in [0, T]$,

$$\begin{aligned} |Y(Z)(t)| \le |Z_0| + \frac{-\tau+1}{Z(\tau)}|\Psi(t, Z(t))| \\ + \frac{\tau}{Z(\tau)\Gamma(\tau)}\int_0^t (t-\eta)^{\tau-1}|\Psi(\eta, Z(\eta))|d\eta, \end{aligned} \tag{126}$$

$$\le |Z_0| + \frac{1-\tau}{Z(\tau)}Z(1, |Z(t)|) + \frac{\tau}{Z(\tau)\Gamma(\tau)}\int_0^t (t-\eta)^{\tau-1}Z(1, |Z(t)|)d\eta, \tag{127}$$

later $Z \in B_{\varpi}$, one can write as

$$\|Y(Z)(t)\| \le |Z_0| + \frac{1-\tau}{Z(\tau)}M(1 + \|Z(t)\|) + \frac{T^{\tau}}{Z(\tau)\Gamma(\tau)}M(1 + \|Z(t)\|), \tag{128}$$

$$\le |Z_0| + \frac{1-\tau}{Z(\tau)}M + \frac{T^{\tau}}{Z(\tau)\Gamma(\tau)}M + [\frac{1-\tau}{Z(\tau)}M + \frac{T^{\tau}}{Z(\tau)\Gamma(\tau)}M]\sigma, \tag{129}$$

$$\le \Delta_2 + \Delta_1\varpi \le \varpi. \tag{130}$$

Now explain as $(YB_{\varpi}) \subset B_{\varpi}$. We will evolve from the mapping Y is shown according to domain. Now consider the sequence $\{Z_n\} \ni Z_n \to Z$ in B_{ϖ} as $n \to \infty$. For all $t \in [0, T]$ we obtain

$$|Y(Z_n(t)) - Y(Z(t))| \tag{131}$$

$$\begin{aligned} \le \frac{1-\tau}{Z(\tau)}|\Psi(t, Z_n(t)) - \Psi(t, Z(t))| \\ + \frac{\tau}{Z(\tau)\Gamma(\tau)}\int_0^t (t-y)^{\tau-1}|\Psi(\eta, Z_n(\eta)) - \Psi(\eta, Z(\eta))|d\eta, \end{aligned} \tag{132}$$

$$\leq \frac{1-\tau}{Z(\tau)}\|\Psi(t,Z_n(t))-\Psi(t,Z(t))\| + \frac{T^\tau}{Z(\tau)\Gamma(\tau)}\|\Psi(\eta,Z_n(\eta))-\Psi(\eta,Z(\eta))\|. \tag{133}$$

The continuous function Ψ: $\|Y(Z_n) - Y(Z)\| \to 0$ as $n \to \infty$ which indicate the operate Y is shown in domain, Thus continuous on B_ϖ.

On B_ϖ we'll note the operation y is equilibrium continuous. Let's do this $Z \in B_\varpi$ and there is $t_1, t_2 \in [0,T]$ with $t_1 < t_2$. Then there's

$$\begin{aligned}&\|Y(Z)(t_2)-Y(Z)(t_1)\|\\ &\leq \frac{1-\tau}{Z(\tau)}|\Psi(t_2,Z(t_2))-\Psi(t_1,Z(t_1))|\\ &\quad+\frac{\tau}{Z(\tau)\Gamma(\tau)}\left\|\left[\int_0^{t_2}(t_2-\eta)^{\tau-1}\right.\right.\\ &\quad\left.\left.-\int_0^{t_1}(t_1-\eta)^{\tau-1}\right]\Psi(\eta,Z(\eta))\,d\eta\right\|.\end{aligned} \tag{134}$$

$$\leq \frac{1-\tau}{Z(\tau)}|\Psi(t_2,Z(t_2))-\Psi(t_1,Z(t_1))| + \frac{\tau M(1+\|Z\|)}{Z(\tau)\Gamma(\tau+1)}(t_2^\tau - t_1^\tau). \tag{135}$$

so the right side $\|YZ(t_2) - YZ(t_1)\|$ goes to zero as $t_2 \to t_1$. According to "Arzelà–Ascoli theorem," the function (YB_ϖ) is relatively compact, so Y is completely continuous. From (2.1), we figure out the solution of our proposed model (4)-(6). □

Theorem 4.5. Assume the function is shown on their domain $\Upsilon \in \mathbb{F}$,and there exist a constant $J > 0 \in |\Upsilon(t,Z) - \Upsilon(t,\widetilde{Z})| \leq J|Z-\widetilde{Z}|$,for all $t \in [0,T]$ and $Z \in \mathbb{F}$, acquiring

$$\frac{(1-\tau)\Gamma(\tau)J + JT^\tau}{Z(\tau)\Gamma(\tau)} < 1, \tag{136}$$

let Z and $\widetilde{Z}$ is a solution of problem (120)

$$\begin{cases} {}^{ABC}D_t^\tau \widetilde{Z}(t) = \Upsilon(t,\widetilde{Z}(t)) \\ \widetilde{Z}(0) = Z_0 + \varepsilon \geq 0, \end{cases} \tag{137}$$

where

$$\begin{cases} \widetilde{Z} = (\widetilde{S},\widetilde{E_1},\widetilde{E_2},\widetilde{I},\widetilde{T},\widetilde{R})^T \\ Z_0+\varepsilon = (S(0)+\varepsilon, E_1(0)+\varepsilon, E_2(0)+\varepsilon, \\ \qquad I(0)+\varepsilon, T(0)+\varepsilon, R(0)+\varepsilon) \\ \Upsilon(t,\widetilde{Z}(t)) = G_i(\widetilde{S},\widetilde{E_1},\widetilde{E_2},\widetilde{I},\widetilde{T},\widetilde{R}), \\ \qquad i = 1,2,3,\ldots,6. \end{cases} \tag{138}$$

The following is accurate.

$$\|Z-\widetilde{Z}\| \leq \left[1 - \frac{(1-\tau)\Gamma(\tau)J + JT^\tau}{Z(\tau)\Gamma(\tau)}\right]^{-1} \times |\varepsilon|. \tag{139}$$

Proof. According to the system's solution, references (120) and (129) are identical to references (122) integral equation

$$\widetilde{Z}(t) = Z_0 + \varepsilon + \frac{1-\tau}{Z(\tau)}\Upsilon(t,\widetilde{Z}(t)) + \frac{\tau}{Z(\tau)\Gamma(\tau)}\int_0^t (t-\eta)^{\tau-1}\Upsilon(\eta,\widetilde{Z}(\eta))\,d\eta. \tag{140}$$

$\forall t \in [0,T]$ we may have

$$|Z(t)-\widetilde{Z}(t)| \leq |\varepsilon| + \frac{-\tau+1}{Z(\tau)}|\Upsilon(t,Z(t)) - \Upsilon(t,\widetilde{Z}(t))| + \frac{\tau}{Z(\tau)\Gamma(\tau)}\int_0^t (t-\eta)^{\tau-1}|\Upsilon(\eta,Z(\eta)) - \Upsilon(\eta,\widetilde{Z}(t))|d\eta, \tag{141}$$

$$\leq |\varepsilon| + \frac{1-\tau}{Z(\tau)}J|Z(t)-\widetilde{Z}(t)| + \frac{\tau}{Z(\tau)\Gamma(\tau)}\int_0^t (t-\eta)^{\tau-1}J|Z(\eta)-\widetilde{Z}(\eta)|\,d\eta. \tag{142}$$

$$\leq |\varepsilon| + \left[\frac{-\tau+1}{Z(\tau)} + \frac{T^\tau}{Z(\tau)\Gamma(\tau)}\right]J\|Z-\widetilde{Z}\|, \tag{143}$$

one may then write

$$\leq |\varepsilon| + \left[\frac{(1-\tau)\Gamma(\tau)+T^\tau}{Z(\tau)\Gamma(\tau)}\right]J\|Z-\widetilde{Z}\|, \tag{144}$$

$$\|Z-\widetilde{Z}\| \leq \left[1 - \frac{J\left[T^\tau + (1-\tau)\Gamma(\tau)\right]}{Z(\tau)\Gamma(\tau)}\right]^{-1}|\varepsilon|. \tag{145}$$

□

Remark 3. If we include $\varepsilon = 0$ in the theorem(4.5), then we'll have the one of a kind answer for the given model (4)-(6).

5. Numerical scheme for the proposed model

This section delves into the details of the suggested model's (5)-(4) approximate solution with the use of the iterative technique of Adams-Bashforth [29] and carry the numerical simulation, the using of the subsidiary condition in addition to the ${}^{ABC}I_0^\tau$ operator, so the model (5)-(4) into fractional integral equations (FIEs)

$$\begin{cases} S(t)-S(0) = & {}^{AB}I_0^\tau K_1(t,S(t)), \\ E_1(t)-E_1(0) = & {}^{AB}I_0^\tau K_2(t,E_1(t)), \\ E_2(t)-E_2(0) = & {}^{AB}I_0^\tau K_3(t,E_2(t)), \\ I(t)-I(0) = & {}^{AB}I_0^\tau K_4(t,I(t)), \\ T(t)-T(0) = & {}^{AB}I_0^\tau K_5(t,T(t)), \\ R(t)-R(0) = & {}^{AB}I_0^\tau K_6(t,R(t)). \end{cases} \tag{146}$$

Provides even more benefits.

$$\begin{aligned}
S(t)-S(0) &= \frac{1-\tau}{Z(\tau)}K_1(S(t),t) \\
&\quad+\frac{\tau}{Z(\tau)\Gamma(\tau)}\int_0^t (t-\eta)^{\tau-1} \\
&\quad K_1(S(\eta),\eta)\,d\eta, \\
E_1(t)-E_1(0) &= \frac{1-\tau}{Z(\tau)}K_2(E_1(t),t) \\
&\quad+\frac{\tau}{Z(\tau)\Gamma(\tau)}\int_0^t (t-\eta)^{\tau-1} \\
&\quad K_2(E_1(\eta),\eta)\,d\eta, \\
E_2(t)-E_2(0) &= \frac{1-\tau}{Z(\tau)}K_3(E_2(t),t) \\
&\quad+\frac{\tau}{Z(\tau)\Gamma(\tau)}\int_0^t (t-\eta)^{\tau-1} \\
&\quad K_3(E_2(\eta),\eta)\,d\eta, \\
I(t)-I(0) &= \frac{1-\tau}{Z(\tau)}K_4(I(t),t) \\
&\quad+\frac{\tau}{Z(\tau)\Gamma(\tau)}\int_0^t (t-\eta)^{\tau-1} \\
&\quad K_4(I(\eta),\eta)\,d\eta, \\
T(t)-T(0) &= \frac{1-\tau}{Z(\tau)}K_5(T(t),t) \\
&\quad+\frac{\tau}{Z(\tau)\Gamma(\tau)}\int_0^t (t-\eta)^{\tau-1} \\
&\quad K_5(T(\eta),\eta)\,d\eta, \\
R(t)-R(0) &= \frac{1-\tau}{Z(\tau)}K_6(R(t),t) \\
&\quad+\frac{\tau}{Z(\tau)\Gamma(\tau)}\int_0^t (t-\eta)^{\tau-1} \\
&\quad K_6(R(\eta),\eta)\,d\eta,
\end{aligned} \tag{147}$$

on frame $t = t_{n+1}$ for $n = 1, 2, 3, \cdots$ into the problem (147), to effect an iterative scheme is dispose:

$$\begin{aligned}
S(t_{n+1})-S(0) &= \frac{1-\tau}{Z(\tau)}K_1(S(t_{n+1}),t_{n+1}) \\
&\quad+\frac{\tau}{Z(\tau)\Gamma(\tau)}\sum_{i=0}^{n}\int_{t_i}^{t_{i+1}} \\
&\quad (t_{n+1}-\eta)^{\tau-1} \\
&\quad K_1(S(\eta),\eta)\,d\eta, \\
E_1(t_{n+1})-E_1(0) &= \frac{1-\tau}{Z(\tau)}K_2(E_1(t_{n+1}),t_{n+1}) \\
&\quad+\frac{\tau}{Z(\tau)\Gamma(\tau)}\sum_{i=0}^{n}\int_{t_i}^{t_{i+1}} \\
&\quad (t_{n+1}-\eta)^{\tau-1} \\
&\quad K_2(E_1(\eta),\eta)\,d\eta, \\
E_2(t_{n+1})-E_2(0) &= \frac{1-\tau}{Z(\tau)}K_3(E_2(t_{n+1}),t_{n+1}) \\
&\quad+\frac{\tau}{Z(\tau)\Gamma(\tau)}\sum_{i=0}^{n}\int_{t_i}^{t_{i+1}} \\
&\quad (t_{n+1}-\eta)^{\tau-1} \\
&\quad K_3(E_2(\eta),\eta)\,d\eta, \\
I(t_{n+1})-I(0) &= \frac{1-\tau}{Z(\tau)}K_4(I(t_{n+1}),t_{n+1}) \\
&\quad+\frac{\tau}{Z(\tau)\Gamma(\tau)}\sum_{i=0}^{n}\int_{t_i}^{t_{i+1}} \\
&\quad (t_{n+1}-\eta)^{\tau-1} \\
&\quad K_4(I(\eta),\eta)\,d\eta, \\
T(t_{n+1})-T(0) &= \frac{1-\tau}{Z(\tau)}K_5(T(t_{n+1}),t_{n+1}) \\
&\quad+\frac{\tau}{Z(\tau)\Gamma(\tau)}\sum_{i=0}^{n}\int_{t_i}^{t_{i+1}} \\
&\quad (t_{n+1}-\eta)^{\tau-1} \\
&\quad K_5(T(\eta),\eta)\,d\eta, \\
R(t_{n+1})-R(0) &= \frac{1-\tau}{Z(\tau)}K_6(R(t_{n+1}),t_{n+1}) \\
&\quad+\frac{\tau}{Z(\tau)\Gamma(\tau)}\sum_{i=0}^{n}\int_{t_i}^{t_{i+1}} \\
&\quad (t_{n+1}-\eta)^{\tau-1} \\
&\quad K_6(R(\eta),\eta)\,d\eta.
\end{aligned} \tag{148}$$

after applying the algebraic expression by using the bi-step interpolating for the adjust function $K_1(S(\beta),\beta)$, $K_2(E_1(\eta),\eta)$, $K_3(E_2(\eta),\eta)$, $K_4(I(\eta),\eta)$, $K_5(T(\eta),\eta)$ and $K_6(R(\eta),\eta)$. On the interval $[t_i, t_{i+1}]$, for $i = 1, 2, \ldots, n$, which are contained within

the IE (148), we obtain

$$\begin{cases} K_1(S(\eta,\eta)) \cong \dfrac{K_1(S(t_i),t_i)}{h}\vartheta + \dfrac{K_1(S(t_{i-1}),t_{i-1})}{h}\kappa, \\ K_2(E_1(\eta,\eta)) \cong \dfrac{K_2(E_1(t_i),t_i)}{h}\vartheta + \dfrac{K_2(E_1(t_{i-1}),t_{i-1})}{h}\kappa, \\ K_3(E_2(\eta,\eta)) \cong \dfrac{K_3(E_2(t_i),t_i)}{h}\vartheta + \dfrac{K_3(E_2(t_{i-1}),t_{i-1})}{h}\kappa, \\ K_4(I(\eta,\eta)) \cong \dfrac{K_4(I(t_i),t_i)}{h}\vartheta + \dfrac{K_4(I(t_{i-1}),t_{i-1})}{h}\kappa, \\ K_5(T(\eta,\eta)) \cong \dfrac{K_5(T(t_i),t_i)}{h}\vartheta + \dfrac{K_5(T(t_{i-1}),t_{i-1})}{h}\kappa, \\ K_6(R(\eta,\eta)) \cong \dfrac{K_6(R(t_i),t_i)}{h}\vartheta + \dfrac{K_6(R(t_{i-1}),t_{i-1})}{h}\kappa. \end{cases} \tag{149}$$

where $\vartheta = t - t_{i-1}$ and $\kappa = t - t_i$.

Above system further shows

$$\begin{cases} S(t_{n+1}) = S(0) + \dfrac{1-\tau}{Z(\tau)}K_1(S(t_n),t_n) + \dfrac{\tau}{Z(\tau)\Gamma(\tau)}\sum_{i=1}^{n}\Big(\dfrac{K_1(S(t_i),t_i)}{h}\lambda + \dfrac{K_1(S(t_{i-1}),t_{i-1})}{h}\mu\Big), \\ E_1(t_{n+1}) = E_1(0) + \dfrac{1-\tau}{Z(\tau)}K_2(E_1(t_n),t_n) + \dfrac{\tau}{Z(\tau)\Gamma(\tau)}\sum_{i=1}^{n}\Big(\dfrac{K_2(E_1(t_i),t_i)}{h}\lambda + \dfrac{K_2(E_1(t_{i-1}),t_{i-1})}{h}\mu\Big), \\ E_2(t_{n+1}) = E_2(0) + \dfrac{1-\tau}{Z(\tau)}K_3(E_2(t_n),t_n) + \dfrac{\tau}{Z(\tau)\Gamma(\tau)}\sum_{i=1}^{n}\Big(\dfrac{K_3(E_2(t_i),t_i)}{h}\lambda + \dfrac{K_3(E_2(t_{i-1}),t_{i-1})}{h}\mu\Big), \\ I(t_{n+1}) = I(0) + \dfrac{1-\tau}{Z(\tau)}K_4(I(t_n),t_n) + \dfrac{\tau}{Z(\tau)\Gamma(\tau)}\sum_{i=1}^{n}\Big(\dfrac{K_4(I(t_i),t_i)}{h}\lambda + \dfrac{K_4(I(t_{i-1}),t_{i-1})}{h}\mu\Big), \\ T(t_{n+1}) = T(0) + \dfrac{1-\tau}{Z(\tau)}K_5(T(t_n),t_n) + \dfrac{\tau}{Z(\tau)\Gamma(\tau)}\sum_{i=1}^{n}\Big(\dfrac{K_5(T(t_i),t_i)}{h}\lambda + \dfrac{K_5(T(t_{i-1}),t_{i-1})}{h}\mu\Big), \\ R(t_{n+1}) = R(0) + \dfrac{1-\tau}{Z(\tau)}K_6(R(t_n),t_n) + \dfrac{\tau}{Z(\tau)\Gamma(\tau)}\sum_{i=1}^{n}\Big(\dfrac{K_6(R(t_i),t_i)}{h}\lambda + \dfrac{K_6(R(t_{i-1}),t_{i-1})}{h}\mu\Big). \end{cases} \tag{150}$$

where $\lambda = I_{i-1,\tau}$ and $\mu = I_{i,\tau}$ are the integral weights defined below in (151), and $Z(\tau)$ denotes the normalization function satisfying $Z(0) = Z(1) = 1$ (see Definition 2.1). so

$$\begin{cases} I_{i-1,\tau} = \int_{t_i}^{t_{i+1}}(t-t_{i-1})(t_{n+1}-t)^{\tau-1}dt, \\ I_{i,\tau} = \int_{t_i}^{t_{i+1}}(t-t_i)(t_{n+1}-t)^{\tau-1}dt, \end{cases} \tag{151}$$

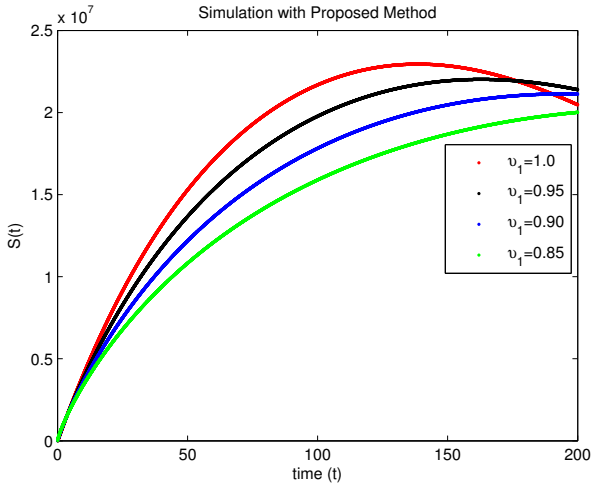

Figure 2: The $S(t)$ population simulation using different fractional order values.

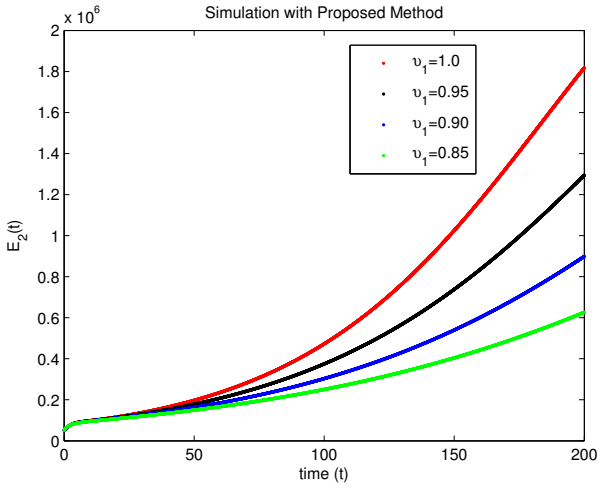

Figure 4: The $E_2(t)$ population simulation using different fractional order values.

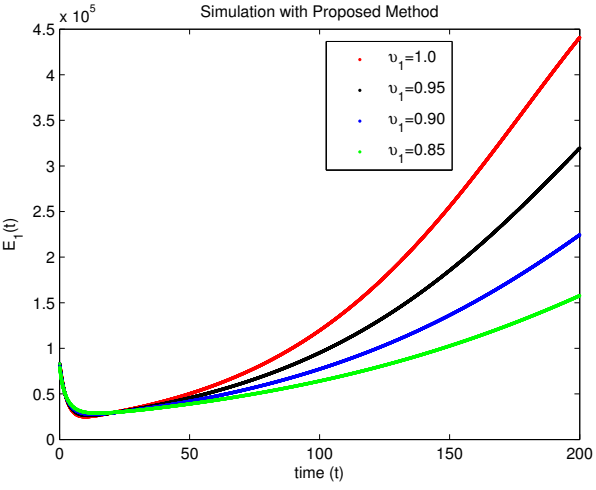

Figure 3: The $E_1(t)$ population simulation using different fractional order values.

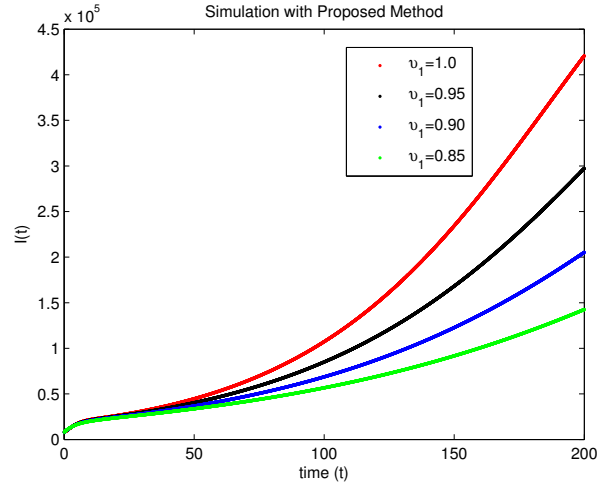

Figure 5: The $I(t)$ population simulation using different fractional order values.

then the simplification of $I_{i-1,\tau}$ and $I_{i,\tau}$ as follows:

$$\begin{cases} I_{i-1,\tau} = -\dfrac{1}{\tau}\left[F - (t_i - t_{i-1})(t_{n+1} - t_i)^{\tau}\right] \\ \qquad\qquad -\dfrac{1}{\tau(\tau-1)} \times \left[\beth - (t_{i+1} - t_i)^{\tau+1}\right], \\ I_{i,\tau} = -\dfrac{1}{\tau}[F] \\ \qquad\qquad -\dfrac{1}{\tau(\tau-1)} \times [\beth - (t_{n+1} - t_i)^{\tau+1}]. \end{cases} \tag{152}$$

where $F = (t_{i+1} - t_{i-1})(t_{n+1} - t_{i+1})^{\tau}$ and $\beth = (t_{n+1} - t_{i+1})^{\tau+1}$.

After placing $t_i = ih$, you can derive that

$$I_{i-1,\tau} = -\frac{h^{\tau+1}}{\tau(\tau+1)}\Big[(n+1-i)^{\tau}(n-i+2+\tau) - (n-i)^{\tau}(n-i+2+2\tau)\Big], \tag{153}$$

$$I_{i,\tau} = \frac{h^{\tau+1}}{\tau(\tau+1)}\Big[(n-i+1)^{\tau+1} - (n-i)^{\tau}(1+n-i+\tau)\Big], \tag{154}$$

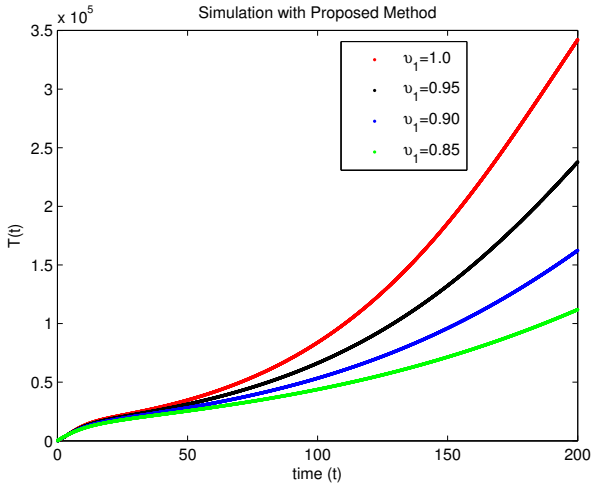

Figure 6: The $T(t)$ population simulation using different fractional order values.

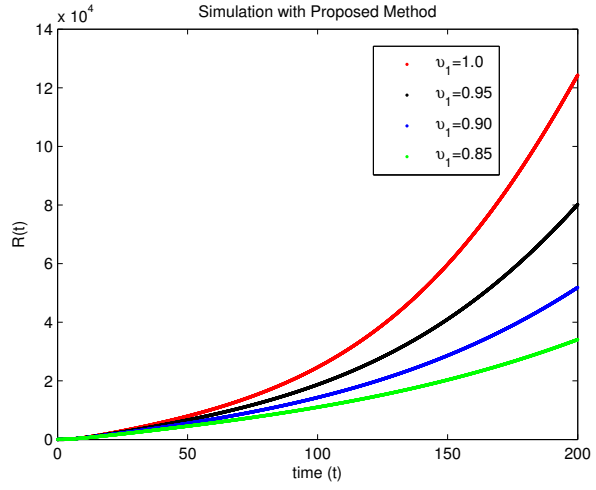

Figure 7: The $R(t)$ population simulation using different fractional order values.

substituting Eq. (153) and Eq. (154) into Eq. (151), so

$$\begin{aligned} S(t_{n+1}) = S(t_0) &+ \frac{1-\tau}{Z(\tau)}[K_1(S(t_n), t_n)] \\ &+ \frac{\tau}{Z(\tau)} \sum_{i=0}^{n} \Big(-\frac{K_1(S(t_n), t_n)}{\tau(\tau+1)} \\ &\times \mathfrak{G} \\ &- (n-i)^{\tau}(n-i+2+2\tau)] \\ &+ \frac{K_1(S(t_{n-1}), t_{n-1})}{\tau(1+\tau)} \\ &\mathfrak{I}] \Big), \end{aligned} \tag{155}$$

Table 3: Comparison of the proposed tuberculosis model with the Caputo-type fractional tuberculosis model of Zhang *et al.* (2021).

Feature	Zhang *et al.* (2021) [28]	Present study
Disease	TB with treatment	TB with multiple exposed populations
Fractional Operator	Caputo derivative	ABC fractional derivative
Memory Effect	Classical Caputo memory	Non-local, non-singular memory kernel
Sensitivity Analysis	Parameter sensitivity discussed via numerical simulation	Comprehensive normalized forward sensitivity indices with explicit sign conditions
Numerical Method	Fractional simulations	Numerical scheme for ABC operator
Fractional-Order Investigation	Limited comparison	Comparison of multiple fractional orders
Novel Contribution	Caputo-based TB model with treatment	ABC-based TB model with dual exposed classes and comprehensive normalized sensitivity analysis

$$\begin{aligned} E_1(t_{n+1}) = E_1(t_0) &+ \frac{-\tau+1}{Z(\tau)}[K_2(E_1(t_n), t_n)] \\ &+ \frac{\tau}{Z(\tau)} \sum_{i=0}^{n} \Big(-\frac{K_2(E_1(t_n), t_n)}{\tau(\tau+1)} \\ &\times \mathfrak{G} \\ &- (n-i)^{\tau}(n-i+2+2\tau)] \\ &+ \frac{K_2(E_1(t_{n-1}), t_{n-1})}{\tau(\tau+1)} \\ &\mathfrak{I}] \Big), \end{aligned} \tag{156}$$

$$\begin{aligned} E_2(t_{n+1}) = E_2(t_0) &+ \frac{1-\tau}{Z(\tau)}[K_3(E_2(t_n), t_n)] \\ &+ \frac{\tau}{Z(\tau)} \sum_{i=0}^{n} \Big(-\frac{K_3(E_2(t_n), t_n)}{\tau(\tau+1)} \\ &\times \mathfrak{G} \\ &- (n-i)^{\tau}(n-i+2+2\tau)] \\ &+ \frac{K_3(E_2(t_{n-1}), t_{n-1})}{\tau(\tau+1)} \\ &\mathfrak{I}] \Big), \end{aligned} \tag{157}$$

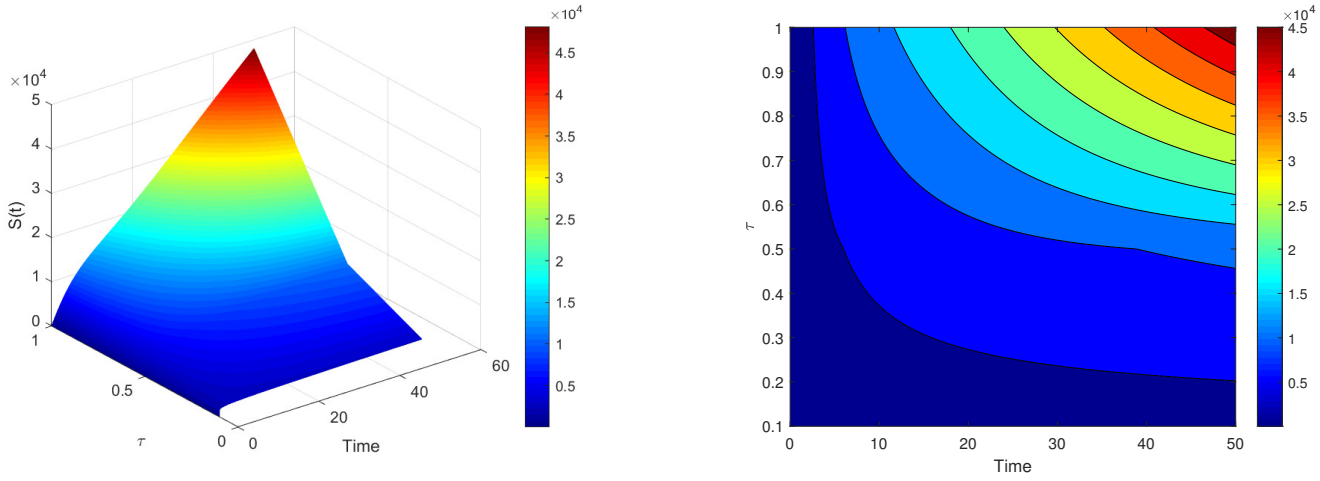

(a) $S(t)$ (b) $S(t)$ at fractional phase

Figure 8: Surface phase simulation of $S(t)$.

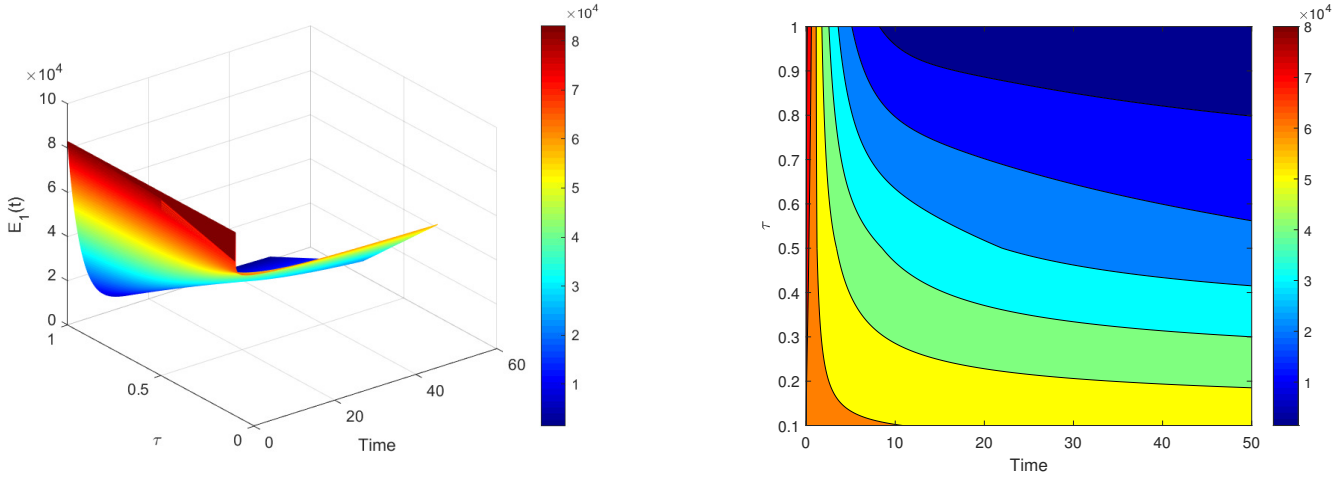

(a) $E_1(t)$ (b) $E_1(t)$ at fractional phase

Figure 9: Surface phase simulation of $E_1(t)$.

$$
\begin{aligned}
I(t_{n+1}) = I(t_0) &+ \frac{1-\tau}{Z(\tau)}[K_4(I(t_n), t_n)] \\
&+ \frac{\tau}{Z(\tau)} \sum_{i=0}^{n} \Big(- \frac{K_4(I(t_n), t_n)}{\tau(\tau+1)} \\
&\times \mathfrak{G} \\
&- (n-i)^{\tau}(n-i+2+2\tau)] \\
&+ \frac{K_4(I(t_{n-1}), t_{n-1})}{\tau(\tau+1)} \\
&\mathfrak{I}\Big),
\end{aligned} \tag{158}
$$

$$
\begin{aligned}
T(t_{n+1}) = T(t_0) &+ \frac{1-\tau}{Z(\tau)}[K_5(T(t_n), t_n)] \\
&+ \frac{\tau}{Z(\tau)} \sum_{i=0}^{n} \Big(- \frac{K_5(T(t_n), t_n)}{\tau(\tau+1)} \\
&\times \mathfrak{G} \\
&- (n-i)^{\tau}(n-i+2+2\tau)] \\
&+ \frac{K_5(T(t_{n-1}), t_{n-1})}{\tau(\tau+1)} \\
&\mathfrak{I}\Big),
\end{aligned} \tag{159}
$$

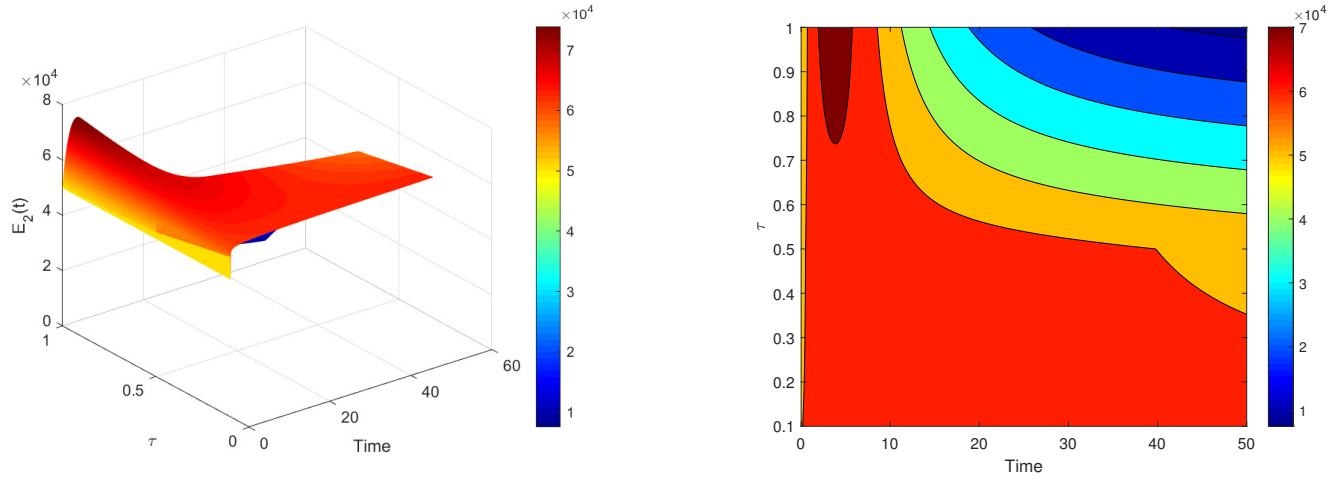

(a) $E_2(t)$ (b) $E_2(t)$ at fractional phase

Figure 10: Surface phase simulation of $E_2(t)$.

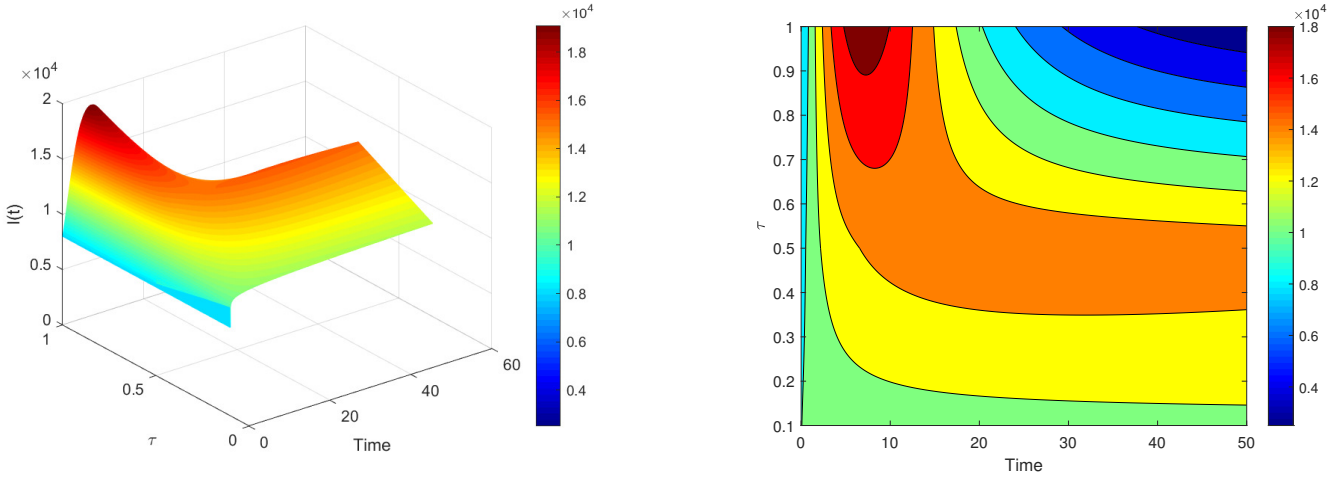

(a) $I(t)$ (b) $I(t)$ at fractional phase

Figure 11: Surface phase simulation of $I(t)$.

$$
\begin{aligned}
R(t_{n+1}) = R(t_0) &+ \frac{-\tau+1}{Z(\tau)}[K_6(R(t_n),t_n)] \\
&+ \frac{\tau}{Z(\tau)}\sum_{i=0}^{n}\Big(-\frac{K_6(R(t_n),t_n)}{\tau(\tau+1)} \\
&\times \mathfrak{G} \\
&- (n-i)^{\tau}(n-i+2+2\tau)] \\
&+ \frac{K_6(R(t_{n-1}),t_{n-1})}{\tau(\tau+1)} \\
&\mathfrak{I}]\Big),
\end{aligned} \tag{160}
$$

where

$$\mathfrak{G} = h^{\tau}[(n+1-i)^{\tau}(n-i+2+\tau)] \tag{161}$$

$$\mathfrak{I} = h^{\tau}[(n+1-i)^{\tau+1} - (n-i)^{\tau}(n-i+1+\tau)] \tag{162}$$

6. Numerical simulations and discussion

Fractional differential equation-based mathematical modeling for the bacterial tuberculosis infection in Khyber Pakhtunkhwa (KPK) is presented. Several fractional orders have been considered in order to conduct an accurate analysis. The parameter values and the initial conditions have been taken from the work of Zhang *et al.* [28]. Based on the above-mentioned initial conditions, the model is formulated using Atangana–Baleanu derivative in the Caputo sense along with Mittag–Leffler function. The simulations show that the dynamics of the model vary depending on different fractional order values. Figures 2–7 illustrate the simulated output for each of the fractional-order values using the ABC technique in determining the effectiveness of active TB infection in the community. The fractional order is an important factor in the memory-dependent system dynamics.

- As can be seen from Figure 2, the population of suscepti-

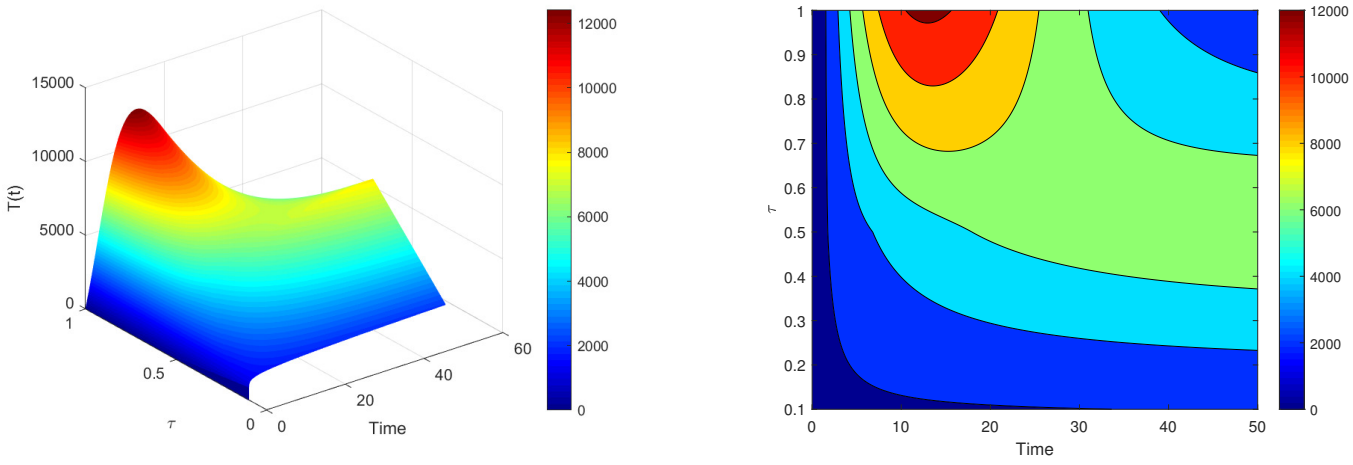

(a) $T(t)$ (b) $T(t)$ at fractional phase

Figure 12: Surface phase simulation of $T(t)$.

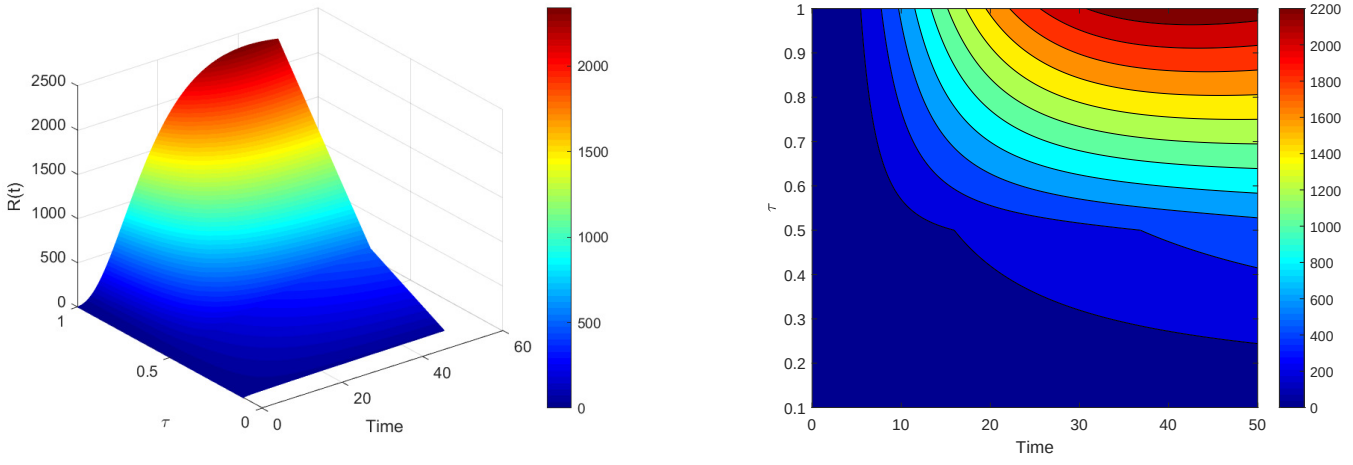

(a) $R(t)$ (b) $R(t)$ at fractional phase

Figure 13: Surface phase simulation of $R(t)$.

bles $S(t)$ decreases steadily with increasing time irrespective of the fractional order. The decrease in the number of susceptible individuals occurs much faster for small values of fractional order, implying that the memory effect hastens the process of depleting the susceptible class.

- In the case of the slowly exposed class $E_1(t)$ (see Figure 3) and the quickly exposed class $E_2(t)$ (see Figure 4), the populations initially start to grow from their initial positions before eventually starting to decrease towards their equilibrium states. This growth is noticeable at higher values of fractional order but the fractional orders show a slower growth before eventually decreasing more rapidly. The exposure population starts to decrease after attaining their maximum value since it is clear that after some time, the infected population becomes stable due to fractional order and treatment.
- Figure 5 depicts the infectious population $I(t)$. It is noticeable that the graph for the infectious population is also showing a trend similar to the exposed classes. In case of higher fractional orders, the graph for infected population goes up by a large amount before dropping, whereas in case of lower fractional orders, there is a controlled increase in the population.
- The treatment population $T(t)$ (Figure 6) will increase in size over time as some members of the exposed and infectious classes move to the treatment and recovered classes respectively. As can be seen, the rate of increase of the treatment population increases with increase in the value of the fractional order, and decreases with decrease in the value of the fractional order due to the lower number of people to be treated. This is because there are fewer infected people.
- Likewise, the recovered population (Figure 7) gradually increases, with the increase being faster in the case of

high fractional order. This trend is comparable to those seen in the exposed and infected population segments.

The most obvious and accurate one is the fractional-order derivative, which has been seen to describe physical phenomena better than the classical-order one. The operators are more efficient when compared to the existing non-integer-order operator. Dynamics of the different fractional-order derivatives are illustrated by the use of numerical results. Table 3 compares the proposed tuberculosis model with the Caputo-type fractional tuberculosis model of Zhang *et al.* [28].

Figures 8, 9, 10, 11, 12, and 13 illustrate the simulation of the three-dimensional surface phase diagram of the suggested fractional-order TB model. From the surface plots, it is observed that all the compartments of the population change smoothly with respect to time using the ABC fractional derivative operator. The susceptible population decreases monotonically, the exposed and infected populations behave like a hump shape with an initial increase, then followed by decrease, and the treatment and recovered populations show a monotonic increase. The fractional order (τ) influences the height of peaks and convergence speed, where small fractional order makes the system stabilize faster. The surfaces confirm that the system converges to a stable endemic equilibrium, validating the analytical stability results.

7. Conclusion

In Pakistan, especially the Khyber Pakhtunkhwa province, the problem of deaths and infections due to tuberculosis persists at a relatively higher level. In order to study the effect of TB and control measures adopted, we have constructed a mathematical model involving slow and fast exposed individuals. The well-posedness of the model was established using the Atangana–Baleanu fractional derivative in the Caputo sense and the Mittag–Leffler kernel. Qualitative analysis was used to analyze the existence of both disease-free equilibrium and endemic equilibria for the stability. The threshold parameter for the disease, $\mathbf{R}_0$, was obtained through the next-generation matrix approach, while sensitivity analysis indicated that the transmission rate β, disease-induced death rate σ_1, and treatment rate γ have the largest absolute normalized sensitivity indices for the parameter values considered. The numerical results obtained via the Adams-Bashforth method have shown that the fractional order τ has a strong effect on the transient behavior of all population compartments. The populations of exposed and infectious individuals initially grow and then decrease to equilibrium, whereas the populations of treatment and recovered individuals grow over time. The above analysis clearly brought out the significance of fractional-order parameter for incorporating memory in the dynamics of disease transmission. However, several drawbacks have been identified. The mathematical model used in the analysis does not consider homogeneous mixing and epidemiological parameters that vary in time and also neglects stochasticity and heterogeneous environment and time-dependent intervention strategies. Additionally, the simulations of the model utilize literature-based parameter values and not clinical data. Future research should consider stochastic, spatially distributed and data-driven fractional-order models.

Data availability

The data supporting the findings of this study are available from the corresponding author upon reasonable request.

Declaration of competing interest

The authors declare no competing interests.

Funding

This research was funded by Prince Sattam bin Abdulaziz University under project number PSAU/2025/01/34222.

Acknowledgment

The authors extend their appreciation to Prince Sattam bin Abdulaziz University for funding this research work through project number PSAU/2025/01/34222.

References

[1] S. Tang & S. B. Squire, "What lessons can be drawn from tuberculosis (TB) control in China in the 1990s? An analysis from a health system perspective", Health Policy **72** (2005) 93. https://doi.org/10.1016/j.healthpol.2004.06.009.

[2] L. J. Podewils, N. Bantubani, C. Bristow, L. E. Bronner, A. Peters, A. Pym & L. D. Mametja, "Completeness and reliability of the Republic of South Africa National Tuberculosis (TB) Surveillance System", BMC Public Health **15** (2015) 765. https://doi.org/10.1186/s12889-015-2117-3.

[3] A. Faustini, A. J. Hall & C. A. Perucci, "Risk factors for multidrug-resistant tuberculosis in Europe: a systematic review", Thorax **61** (2006) 158. https://doi.org/10.1136/thx.2005.045963.

[4] S. Tang, L. Wang, H. Wang & D. P. Chin, "Access to and affordability of healthcare for TB patients in China: issues and challenges", Infectious Diseases of Poverty **5** (2016) 10. https://doi.org/10.1186/s40249-016-0096-y.

[5] J. R. Glynn, J. Bauer, A. S. de Boer, M. W. Borgdorff, P. E. M. Fine, P. Godfrey-Faussett & E. Vynnycky, "Interpreting DNA fingerprint clusters of *Mycobacterium tuberculosis*. European Concerted Action on Molecular Epidemiology and Control of Tuberculosis", International Journal of Tuberculosis and Lung Disease **3** (1999) 1055. Available online: https://pubmed.ncbi.nlm.nih.gov/10599007/.

[6] T. T. Tsai, C. Y. Huang, C. A. Chen, S. W. Shen, M. C. Wang, C. M. Cheng & C. F. Chen, "Diagnosis of tuberculosis using colorimetric gold nanoparticles on a paper-based analytical device", ACS Sensors **2** (2017) 1345. https://doi.org/10.1021/acssensors.7b00450.

[7] P. Narasimhan, J. Wood, C. R. MacIntyre & D. Mathai, "Risk factors for tuberculosis", Pulmonary Medicine **2013** (2013) 828939. https://doi.org/10.1155/2013/828939.

[8] K. Lönnroth, G. Roglic & A. D. Harries, "Improving tuberculosis prevention and care through addressing the global diabetes epidemic: from evidence to policy and practice", The Lancet Diabetes & Endocrinology **2** (2014) 730. https://doi.org/10.1016/S2213-8587(14)70109-3.

[9] P. Nadol, K. W. Stinson, W. Coggin, M. Naicker, C. D. Wells, B. Miller & L. J. Nelson, "Electronic tuberculosis surveillance systems: a tool for managing today's TB programs", International Journal of Tuberculosis and Lung Disease **12** (2008) S8. Available online: https://pubmed.ncbi.nlm.nih.gov/18302816/.

[10] K. Floyd, "Costs and effectiveness—the impact of economic studies on TB control", Tuberculosis **83** (2003) 187. https://doi.org/10.1016/S1472-9792(02)00077-X.

[11] D. Garijo, S. Kinnings, L. Xie, L. Xie, Y. Zhang, P. E. Bourne & Y. Gil, "Quantifying reproducibility in computational biology: the case of the tuberculosis drugome", PLoS ONE **8** (2013) e80278. https://doi.org/10.1371/journal.pone.0080278.

[12] M. Farman, A. Hasan, M. U. Sultan, A. Ahmad, A. Akgül, F. Chaudhry, M. Zakarya, W. Albalawi & W. Weera, "Yellow virus epidemiological analysis in red chili plants using Mittag–Leffler kernel", Alexandria Engineering Journal **66** (2023) 811. https://doi.org/10.1016/j.aej.2022.10.064.

[13] A. Sajjad, M. Farman, A. Hasan & K. S. Nisar, "Transmission dynamics of fractional-order yellow virus in red chili plants with the Caputo–Fabrizio operator", Mathematics and Computers in Simulation **207** (2023) 347. https://doi.org/10.1016/j.matcom.2023.01.004.

[14] C. Xu, M. Farman, A. Hasan, A. Akgül, M. Zakarya, W. Albalawi & C. Park, "Lyapunov stability and wave analysis of COVID-19 Omicron variant of real data with fractional operator", Alexandria Engineering Journal **61** (2022) 11787. https://doi.org/10.1016/j.aej.2022.05.025.

[15] M. A. Khan & A. Atangana, "Mathematical modeling and analysis of COVID-19: a study of new variant Omicron", Physica A: Statistical Mechanics and its Applications **599** (2022) 127452. https://doi.org/10.1016/j.physa.2022.127452.

[16] M. Farman, M. U. Saleem, A. Ahmad & M. O. Ahmad, "Analysis and numerical solution of SEIR epidemic model of measles with non-integer time fractional derivatives by using Laplace Adomian decomposition method", Ain Shams Engineering Journal **9** (2018) 3391. https://doi.org/10.1016/j.asej.2017.11.010.

[17] M. Caputo & M. Fabrizio, "A new definition of fractional derivative without singular kernel", Progress in Fractional Differentiation and Applications **1** (2015) 73. https://doi.org/10.12785/pfda/010201.

[18] J. Losada & J. J. Nieto, "Properties of a new fractional derivative without singular kernel", Progress in Fractional Differentiation and Applications **1** (2015) 87. https://doi.org/10.12785/pfda/010202.

[19] S. Bhatter, S. Kumawat, S. D. Purohit & D. L. Suthar, "Mathematical modeling of tuberculosis using Caputo fractional derivative: a comparative analysis with real data", Scientific Reports **15** (2025) 12672. https://doi.org/10.1038/s41598-025-97502-5.

[20] B. C. Agbata, R. Dervishi, D. F. Agbebaku, E. Cenaj, O. C. Collins, A. U. Ezeafulukwe, M. M.-A. Shior & G. C. E. Mbah, "A comprehensive analysis of fractional-order model of tuberculosis with treatment intervention", BMC Infectious Diseases **25** (2025) 1070. https://doi.org/10.1186/s12879-025-11303-9.

[21] A. O. Sangotola, S. B. Adeyemo, O. A. Nuga, A. E. Adeniji & A. J. Adigun, "A tuberculosis model with three infected classes", Journal of the Nigerian Society of Physical Sciences **6** (2024) 1881. https://doi.org/10.46481/jnsps.2024.1881.

[22] O. F. Lawal & A. Abidemi, "Modelling the effect of vaccination on the dynamics of tuberculosis in an age-structured population", Proceedings of the Nigerian Society of Physical Sciences **2** (2025) 179. https://doi.org/10.61298/pnspsc.2025.2.179.

[23] J. F. Gómez-Aguilar, "New bilingualism model based on fractional operators with Mittag–Leffler kernel", The Journal of Mathematical Sociology **41** (2017) 172. https://doi.org/10.1080/0022250X.2017.1356828.

[24] M. Ozair, T. Hussain, A. Aslam, R. Anees, M. Tanveer & J. F. Gómez-Aguilar, "Management of pine forests by assessment of insect pests and nematodes", The European Physical Journal Plus **136** (2021) 916. https://doi.org/10.1140/epjp/s13360-021-01934-7.

[25] Z. Yang, M. Xiao, Z. Wang, Y. Sun, X. Yang, J. F. Gómez-Aguilar & J. Cao, "Higher-order interactions in the spatio-temporal dynamics of Leslie–Gower predator–prey systems", Computational and Applied Mathematics **45** (2026) 344. https://doi.org/10.1007/s40314-026-03740-2.

[26] A. Atangana, "Modelling the spread of COVID-19 with new fractal-fractional operators: can the lockdown save mankind before vaccination?", Chaos, Solitons & Fractals **136** (2020) 109860. https://doi.org/10.1016/j.chaos.2020.109860.

[27] M. Farman, A. Akgül, S. F. Aldosary, K. S. Nisar & A. Ahmad, "Fractional-order model for complex Layla and Majnun love story with chaotic behaviour", Alexandria Engineering Journal **61** (2022) 6725. https://doi.org/10.1016/j.aej.2021.12.018.

[28] X. H. Zhang, A. Ali, M. A. Khan, M. Y. Alshahrani, T. Muhammad & S. Islam, "Mathematical analysis of the TB model with treatment via Caputo-type fractional derivative", Discrete Dynamics in Nature and Society **2021** (2021) 9512371. https://doi.org/10.1155/2021/9512371.

[29] M. Toufik & A. Atangana, "New numerical approximation of fractional derivative with non-local and non-singular kernel: application to chaotic models", The European Physical Journal Plus **132** (2017) 444. https://doi.org/10.1140/epjp/i2017-11717-0.